Technical Companion to TFPT

Conventions, Positivity, APS Interfaces, and Comparison Maps

Stefan Hamann Alessandro Rizzo

Companion document for the TFPT 4.5 paper series – April 27, 2026

Abstract

The Technical Companion is the long toolbox for the TFPT paper series. It holds conventions, analytic interfaces, auxiliary proofs, extended comparison maps, empirical ledgers, optional continuations, record algebra, horizon material, transient channels, and the E8 stage atlas. It is not a stand-alone theorem paper and should not be required reading for the primitive kernel or the carrier theorem.

Scope box: inputs, contribution, non-claims, audit surface

Inputs from previous papers. The entire TFPT 4.5 paper series.
New theorem contribution. None by default. Companion material can support theorem papers, but new claims should be promoted into the appropriate paper rather than hidden here.
Not claimed here. The companion does not replace Papers 1–6 and does not elevate comparison maps or optional continuations to theorem status.
Falsification or audit surface. The companion fails if it blurs theorem, standard-theorem interface, empirical comparison, optional continuation, and programmatic target language.

Contents

1 Purpose

The companion exists to keep the six papers short enough to be reviewed by the right audiences. A reader checking the carrier theorem should not be forced to read CMB sky maps, E8 scale grammar, record algebra, or horizon continuations.

2 Core Convention Blocks

The first part collects:

- symbol guide,
- relative objects,
- layered datum and admissibility conventions,
- APS and superconnection setup,
- positivity conventions,
- theorem-status vocabulary.

3 Analytic Backend

This part holds expanded details for:

- relative reflection positivity with fermions,
- admissible OS reconstruction,
- asymptotic scattering,
- dressed massless interface,
- exact admissible flow and 1PI expansion details,
- Yukawa kernels and positivity lemmas.

4 Comparison Backend

This part holds:

- constants atlas,
- extended benchmarks,
- compact and full empirical ledgers,
- residual readout and interface refinements,
- operational prediction matrix,
- target and kill-test rows,
- novelty boundary and literature positioning.

5 Downstream and Optional Continuations

This part holds material that should not drive the primitive theorem chain:

- E8 stage atlas,
- optional arithmetic continuations,
- infrared seam-transfer continuations,
- horizon continuations,
- record algebra and pointer dynamics,
- information-theoretic readings,
- cut-and-project readings,
- transient event channels.

6 Main Technical Development

This section contains the main technical development assigned to this paper by the TFPT 4.5 clean split. Cross-paper background is referenced through dependency and scope boxes; extended backend material is kept in the Technical Companion.

7 Downstream closure modules from the closed branch

The present section records the downstream closure modules that start from the already fixed branch object

$$\mathfrak{T}_\star, \qquad \Gamma^{\mathrm{ren}}_{\mathrm{TFPT}}, \qquad (\mathcal{H}_{\mathrm{adm}}, \mathfrak{A}_{\mathrm{adm}}), \qquad (\Lambda_{\mathrm{IR}}, N_{\mathrm{DW}}, \theta_i, T_R, \mathcal{I}_{\mathrm{LG}}).$$

Nothing in this section changes the upstream theorem chain. The exact proof status of these downstream closures is recorded in the proof-obligation ledger, and each statement below is phrased only as far as it factors through already fixed branch data. The stationary geometric scale, boundary-spectral Planck normalization, and Schwarzschild–de Sitter vacuum branch have been promoted to the main theorem surface in [TFPT cross-reference: `thm:absolute-spectral-planck-closure`]; every subsection collected here is therefore genuinely status **[P]**.

7.1 [P] Stationary horizons, modular thermality, and compact objects

Conjecture 7.1 (Modular horizon thermality on the admissible branch)**.** Assume the split property and stationarity of the exterior wedge algebra on the vacuum branch. Then for the outside algebra one has

$$\Delta^{it}_{\mathcal{A}_{\mathrm{out}}} = e^{-2\pi t K_H},$$

where K_H is the horizon modular generator. Hence the reduced outside state is KMS and the horizon temperature is

$$T_H = \frac{\kappa}{2\pi}.$$

Remark (Programmatic proof route). The intended route upgrades the split inclusion theorem Theorem 18.1 to a stationary modular setting and then applies the admissible local net reconstruction on the exterior algebra. This route is recorded here as a closure target, not as a completed proof.

Conjecture 7.2 (Hawking temperature on the stationary branch)**.** For the static vacuum branch of [TFPT cross-reference: `cor:schwarzschild_de_sitter_vacuum_branch`], the horizon temperature is

$$T_H = \frac{1}{4\pi r_h}\left(1 - \Lambda_{\mathrm{IR}} r_h^2\right).$$

Conjecture 7.3 (Wald entropy on the scalaron corrected branch)**.** On the same branch the entropy is

$$S_W = \frac{A}{4G_N}\left(1 + \frac{R_h}{3M^2}\right).$$

Conjecture 7.4 (Kerr branch and compact object corrections)**.** The stationary rotating branch is Kerr de Sitter at leading order, with compact object corrections of size

$$\Delta\eta,\ \Delta r_{\mathrm{ISCO}} = O\left(\frac{1}{M^2 r_g^2}\right) + O(\Lambda_{\mathrm{IR}} r_g^2).$$

Conjecture 7.5 (Tensor and scalaron wave channel closure)**.** The gravitational wave sector on the closed branch consists of the massless tensor channel and the positive scalaron channel. The tensor speed satisfies

$$c_T = 1,$$

and the phase correction has the form

$$\Delta\Psi(f) = O\left(\frac{f^2}{M^2}\right) + O\big(\rho(U_\Sigma)\big).$$

7.2 [P] Primordial perturbation closure and CMB transfer

Conjecture 7.6 (Reheating fixed e fold number)**.** The number of e folds on the closed branch is fixed by

$$N_* := 57.1 + \frac{1}{4}\ln\frac{V_*}{M_{Pl}^4} + \frac{1}{4}\ln\frac{V_*}{\rho_{\rm end}} - \frac{1-3w_{\rm reh}}{12(1+w_{\rm reh})}\ln\frac{\rho_{\rm reh}}{\rho_{\rm end}},$$

where the closed-branch reheating density $\rho_{\rm reh}$ is determined by the branch reheating scale T_R, and the constant 57.1 absorbs the standard pivot conversion $67 - \ln(k_*/(a_0H_0))$ at $k_* = 0.05/\mathrm{Mpc}$. The combined V_* kernel $(1/4)\ln(V_*^2/(M_{Pl}^4\rho_{\rm end}))$ is the standard Liddle–Leach form [7]; the sign of the V_*/M_{Pl}^4 term as it appeared in the previous manuscript revision was inconsistent with the chi-square Stage 1 cross-check by approximately ten e-folds and has been corrected.

Conjecture 7.7 (Primordial mode closure from the seam state)**.** Scalar and tensor perturbations obey

$$v_k'' + \left(k^2 - \frac{z''}{z}\right)v_k = 0, \qquad u_k'' + \left(k^2 - \frac{a''}{a}\right)u_k = 0,$$

with Bogoliubov coefficients determined by the seam transfer spectrum

$$\beta_k = \mathcal{F}_k\big(\{\lambda_j(U_\Sigma)\}\big).$$

Hence

$$\mathcal{P}_{\mathcal{R}}(k) = \mathcal{P}_{\mathcal{R}}^{\rm St}(k)|\alpha_k + \beta_k|^2.$$

Conjecture 7.8 (CMB transfer closure on the closed branch (Stage 1: spectra))**.** Given the primordial spectrum of Conjecture 7.7, the CMB angular spectra are

$$C_\ell^{XY} = 4\pi\int\frac{dk}{k}\,\mathcal{P}_{\mathcal{R}}(k)\,\Delta_\ell^X(k)\Delta_\ell^Y(k).$$

The transfer kernels Δ_ℓ^X are determined by the same branch background and the standard linearized recombination hierarchy. At Stage 1 the closed-branch input is therefore the admissible spectrum $\{\lambda_j(U_\Sigma)\}$ alone, and the resulting closure

$$\{\lambda_j(U_\Sigma)\} \implies \mathcal{P}_{\mathcal{R}}(k) \implies C_\ell^{XY}$$

fixes the angular statistics but not a specific sky realization.

Conjecture 7.9 (Ergodic microcanonical seam lift (Stage 2: map))**.** Let $U_\Sigma\psi_j = \lambda_j\psi_j$ be the admissible eigenpairs of the seam transfer operator and let u_Σ be the closed-branch seam state of the rigid object $\mathfrak{T}_\star$. Let $\mathcal{W}_\Sigma$ denote the canonical seam scrambler, defined *not* as a power limit of U_Σ on the admissible state—which would, by the Perron–Frobenius mechanism on a positive trace-class operator with spectral gap, collapse onto the leading eigenvector and

produce no shell-level ergodicity—but as the *projective modular trace cocycle* associated with the seam-transfer dynamics:

$$\mathcal{W}_\Sigma : \ (\ell, r, s) \ \longmapsto \ \mathfrak{c}_{\ell,r}^{(s)} \in \mathbb{F}_{p_\ell}^4, \qquad \mathfrak{c}_{\ell,r}^{(s)} := \big(A_{\ell,r}^{(s)}, B_{\ell,r}^{(s)}, C_{\ell,r}^{(s)}, D_{\ell,r}^{(s)}\big),$$

where each component is a reduced trace of a word in the canonical operator algebra $\langle U_\Sigma, P_{\mathrm{adm}}, \tau_{\mathrm{dbl}}, \iota_C, U_5, U_6\rangle$ acting on the admissible representation V_{adm}:

$$A_{\ell,r}^{(s)} = \mathrm{red}_{p_\ell} \mathrm{Tr}\big(P_{\mathrm{adm}}\, \mathcal{O}_{\ell,r,A}^{(s)}\big), \quad \mathcal{O}_{\ell,r,X}^{(s)} \in \langle U_\Sigma, \tau_{\mathrm{dbl}}, \iota_C, U_5, U_6\rangle,$$

and similarly for B, C, D. The variant index $s \in \{1, 2\}$ generates the double-digit lift to p_ℓ^2 resolution of [TFPT cross-reference: `rem:finite-field-seam-mixer`], and the variant index $r \in \{0, 1, 2\}$ generates the three streams $g_{\ell 0}^\star$, $\mathrm{Re}\, g_{\ell m}^\star$, $\mathrm{Im}\, g_{\ell m}^\star$. Define the closed-branch *ergodic shell vector*

$$g_{\ell m}^\star := \langle e_{\ell m}, \mathcal{W}_\Sigma u_\Sigma\rangle$$

through the trace-tower formulae of [TFPT cross-reference: `rem:finite-field-seam-mixer`], and the *microcanonical normalization* per multipole shell

$$\boxed{a_{\ell m}^{T,\star} := \sqrt{(2\ell+1)\, C_\ell^\star}\ \frac{g_{\ell m}^\star}{\sqrt{|g_{\ell 0}^\star|^2 + 2\sum_{m=1}^{\ell} |g_{\ell m}^\star|^2}}}$$

with $C_\ell^\star$ the Stage 1 spectrum of [TFPT cross-reference: `thm:cmb_transfer_closure_closed_branch`]. Then the realized sky is

$$\frac{\Delta T^\star}{T_0}(\hat{n}) = \sum_{\ell m} a_{\ell m}^{T,\star}\, Y_{\ell m}(\hat{n}).$$

By construction the shell quotient enforces $C_\ell^{\mathrm{rec}} = C_\ell^\star$ exactly per multipole. The Stage 2 closure

$$\big(\{\lambda_j(U_\Sigma)\}, u_\Sigma, \mathcal{W}_\Sigma\big) \implies \{g_{\ell m}^\star\} \implies \{a_{\ell m}^{T,\star}\} \implies \Delta T^\star(\hat{n})$$

upgrades the Stage 1 statistical closure to a deterministic sky realization on the closed branch.

Remark (Ergodicity replaces the integrable phase formula). A scalar phase law of the form

$$\Theta_{\ell m} = A + B(\ell^2 + \ell + m) + C\ell + Dm \pmod{2\pi},$$

constructed from finitely many closure scalars, is necessarily separable in (ℓ, m) and therefore *integrable*: the inner-shell phase difference $\Theta_{\ell,m+k} - \Theta_{\ell,m}$ is independent of m, and the discrete decorrelation amplitude

$$A_\ell(k) := \Big|\sum_m e^{i(\Theta_{\ell,m+k} - \Theta_{\ell,m})}\Big|$$

grows linearly, $A_\ell(k) = O(\ell)$. The realized sky then carries coherent stripe / ray artefacts and a heavy-tailed pixel histogram (excess kurtosis $g_2 \gtrsim 5$). Numerical evidence on the closed-branch carrier wheel rules this scalar regime out at the level of Planck Gaussianity.

The *ergodic microcanonical seam lift* of [TFPT cross-reference: `thm:cmb_seam_phase_realization`] replaces the scalar phase law by a vector lift on each $(2\ell+1)$-dimensional shell. Concentration of measure on the $(2\ell+1)$-sphere $S^{2\ell}$ yields $A_\ell(k) = O(\sqrt{\ell})$ and pixel Gaussianity at the central limit level. The seam scrambler $\mathcal{W}_\Sigma$ is the structural object that enforces this ergodicity.

Remark (Finite-field seam mixer with trace reduction). A theorem-friendly explicit realization of the seam scrambler is given by a finite-field rational phase function whose coefficients arise from *reduced traces of canonical TFPT operator products* on the admissible representation, not from a numerical hash of the closure key.

For each multipole shell choose a prime

$$p_\ell \;\geq\; 2\ell+1,$$

and define, on the admissible finite-dimensional representation V_{adm} of dimension $N = \Omega_{\mathrm{adm}}$,

$$A_{\ell,r} := \mathrm{red}_{p_\ell}\,\mathrm{Tr}\big(P_{\mathrm{adm}}\,U_\Sigma^{\ell+r}\,U_5^{r}\big), \qquad B_{\ell,r} := \mathrm{red}_{p_\ell}\,\mathrm{Tr}\big(P_{\mathrm{adm}}\,U_\Sigma^{\ell}\,U_6^{r}\big), \tag{1}$$

$$C_{\ell,r} := \mathrm{red}_{p_\ell}\,\mathrm{Tr}\big(P_{\mathrm{adm}}\,\tau_{\mathrm{dbl}}\,U_\Sigma^{\ell+r}\big), \qquad D_{\ell,r} := \mathrm{red}_{p_\ell}\,\mathrm{Tr}\big(P_{\mathrm{adm}}\,\iota_{\mathrm{C}}\,U_\Sigma^{\ell}\big), \tag{2}$$

with U_5, U_6 the carrier-rank generators of [TFPT cross-reference: `thm:cosmology-closure`] and the carrier algebra. Set $x := m+\ell+1 \pmod{p_\ell}$ and

$$f_{\ell,r}(x) := A_{\ell,r}x + B_{\ell,r}x^{-1} + C_{\ell,r}x^2 + D_{\ell,r}\,\ell\,x^3 \quad \text{in } \mathbb{F}_{p_\ell},$$

with the p_ℓ^2-resolved double-digit lift to a uniform sample on $(0,1)$,

$$u_{\ell m}^{(r)} := \frac{p_\ell\, f_{\ell,r,1}(x) + f_{\ell,r,2}(x) + \frac{1}{2}}{p_\ell^2},$$

where $f_{\ell,r,1}, f_{\ell,r,2}$ are two independent admissible variants of the trace recipe. The deterministic complex normal vector is then

$$g^\star_{\ell 0} := \Phi^{-1}\big(u^{(0)}_{\ell 0}\big), \quad g^\star_{\ell m} := \frac{\Phi^{-1}\big(u^{(1)}_{\ell m}\big) + i\Phi^{-1}\big(u^{(2)}_{\ell m}\big)}{\sqrt{2}} \quad (m \geq 1),$$

to which the microcanonical normalization of [TFPT cross-reference: `thm:cmb_seam_phase_realization`] is applied shell by shell. The architecture

finite-field coefficients = reduced traces of canonical TFPT operators

makes the seam mixer a closed-branch object: the only inputs are the operator algebra $(U_\Sigma, P_{\mathrm{adm}}, \tau_{\mathrm{dbl}}, \iota_{\mathrm{C}}, U_5, U_6)$ on V_{adm}, the closed-branch eigenvalue data, and elementary integer arithmetic.

Lemma 7.10 (Decorrelation bound from incomplete Weil sums)**.** *Fix $\ell \geq 2$ and $1 \leq k \leq \ell$. Let $f_{\ell,r} \in \mathbb{F}_{p_\ell}(x)$ be a non-zero rational phase function of total degree D as in* [TFPT cross-reference: `rem:finite-field-seam-mixer`]*, and assume the shifted difference*

$$\Delta_k f_{\ell,r}(x) := f_{\ell,r}(x+k) - f_{\ell,r}(x) \in \mathbb{F}_{p_\ell}(x)$$

is non-constant on $\mathbb{F}_{p_\ell}^\times$ and not Artin–Schreier degenerate, i.e. does not admit a representation $\Delta_k f = g^{p_\ell} - g + \mathrm{const}$ with $g \in \mathbb{F}_{p_\ell}(x)$. Then the complete *exponential sum obeys the Weil estimate of Bombieri [8] and Deligne [9],*

$$\Big|\sum_{x\in\mathbb{F}_{p_\ell}^\times} e^{2\pi i\,\Delta_k f_{\ell,r}(x)/p_\ell}\Big| \;\leq\; (D-1)\sqrt{p_\ell}.$$

The discrete decorrelation amplitude of the realised seam lift is, however, the incomplete *sum over the integer interval $1 \leq m \leq \ell$,*

$$A_\ell(k) = \Big|\sum_{m=1}^{\ell} e^{2\pi i\,\Delta_k f_{\ell,r}(m+\ell+1)/p_\ell}\Big|.$$

Combining the complete-sum bound with the standard Pólya–Vinogradov [10] completion procedure yields the incomplete-sum estimate

$$A_\ell(k) \;\le\; C_D\,\sqrt{p_\ell}\,\log p_\ell \;=\; O\big(\sqrt{\ell}\,\log \ell\big),$$

with a constant C_D depending only on the total degree D of $f_{\ell,r}$. Pixel Gaussianity of the realized sky follows by the central limit theorem on the $(2\ell+1)$-dimensional admissible shell. In particular, the scalar phase law $\Theta_{\ell m} = A + B(\ell^2+\ell+m) + C\ell + Dm \pmod{2\pi}$ violates the non-constancy hypothesis (its shifted difference is identically zero in m), the bound does not apply to it, and the empirical $A_\ell(k) \sim \ell$ scaling of [TFPT cross-reference: `rem:ergodic-vs-scalar`] *is consistent with that violation. The logarithmic factor in the bound is harmless for all diagnostics (it is dominated by the square-root growth at the multipole resolutions reachable by Planck) but mathematically essential: the realized sums are incomplete, and the Weil estimate alone applies only to the completion.*

Remark (Open obligation O_{20a} at the operator level). The trace-reduction architecture of [TFPT cross-reference: `rem:finite-field-seam-mixer`] reduces the canonical lift obligation to a purely operator-theoretic statement: O_{20a} asks for the closed-form derivation of the operator algebra $(U_\Sigma, P_{\mathrm{adm}}, \tau_{\mathrm{dbl}}, \iota_{\mathrm{C}}, U_5, U_6)$ on V_{adm} from the seam-transfer dynamics of $\mathfrak{T}_\star$. Once those operators are explicitly given, the trace formulae of [TFPT cross-reference: `rem:finite-field-seam-mixer`] produce the seam scrambler $\mathcal{W}_\Sigma$ deterministically, and the Weil bound of Lemma 7.10 promotes the ergodicity claim from a numerical observation to a theorem.

Remark (Multiplicity audit). The trace formulae of [TFPT cross-reference: `rem:finite-field-seam-mixer`] are not unique: any admissible permutation or integer-power perturbation of the operator strings $(P_{\mathrm{adm}}, U_\Sigma^{\ell+r}, U_5^r, \tau_{\mathrm{dbl}}, \iota_{\mathrm{C}}, U_6^r)$ yields a valid trace recipe in the same canonical class. A robust Stage 2 lift must give a Gaussian-typical sky for *every* member of this class, not just a hand-picked combination. Numerical evidence on four mutually inequivalent trace variants (default; $U_5 \leftrightarrow U_6$ swap; squared inclusions $\tau_{\mathrm{dbl}} \to \tau_{\mathrm{dbl}}^2, \iota_{\mathrm{C}} \to \iota_{\mathrm{C}}^2$; full carrier product $U_5^r U_6^r$) shows that the pixel moments, per-ℓ KS test, parity asymmetry, and Gaussian-baseline correlation r_ℓ all sit at the Gaussian-baseline level for every variant, with pairwise variant–variant correlations inside the same $\pm 1/\sqrt{2\ell+1}$ envelope. This multiplicity audit rules out the cherry-pick objection.

Remark (Status of the two CMB closure stages). [TFPT cross-reference: `thm:cmb_transfer_closure_closed_bra` (*Stage 1: spectra*) and [TFPT cross-reference: `thm:cmb_seam_phase_realization`] (*Stage 2: map*) are complementary, not equivalent. Stage 1 explains the angular statistics of the CMB from $\{\lambda_j(U_\Sigma)\}$ alone; Stage 2 in addition predicts a specific sky realization, conditional on the seam state u_Σ being treated as a determinate datum of $\mathfrak{T}_\star$ rather than as a sampled element of an ensemble. The compressed slogan is

$$\text{eigenvalues} \;\Rightarrow\; \text{spectra}, \qquad \text{eigenvalues} + \text{seam phases} \;\Rightarrow\; \text{sky realization}.$$

Falsification path. Stage 1 is killed by any robust deviation of the angular spectra from the admissible-branch transfer of $\{\lambda_j(U_\Sigma)\}$. Stage 2 is killed independently if any $a_{\ell m}^{T,\star}$ obtained from $\Theta_j = \arg\langle \psi_j, u_\Sigma\rangle$ disagrees with the measured Planck $a_{\ell m}^T$ at a level exceeding cosmic variance plus the determinant-bound slack of [TFPT cross-reference: `cor:ir-seam-transfer-bounds`].

Remark (Three open obligations of the Stage 2 closure). The Stage 2 statement [TFPT cross-reference: `thm:cmb_seam_phase_realization`] carries three named obligations that must be discharged before the conjecture can be promoted to a theorem-level deterministic sky prediction:

(O1) **Canonical seam-state lift.** The closed-branch determinant-line phase $[u_\Sigma]$ must be lifted to a determinate element of the spectral basis $\{\psi_j\}$ of U_Σ on a finite-mode truncation,

in such a way that the lift uses only data internal to $\mathfrak{T}_\star$. The ergodic block lift of [TFPT cross-reference: `thm:cmb_seam_phase_realization`] provides the correct *type* for this lift; what remains is a closed-form description of the seam scrambler $\mathcal{W}_\Sigma$ itself, derived from the seam-transfer dynamics rather than approximated by a counter-based mixer.

(O2) **SO(3) orientation gauge.** The boundary content of the closed branch as recorded in the present version is rotation invariant: no canonical sky triad is selected. The deterministic prediction is therefore strictly $\{a_{\ell m}^{T,\star}\}/\mathrm{SO}(3)$, and only rotation invariant diagnostics (C_ℓ, parity asymmetry, peak ratios, multipole amplitude pattern, Gaussianity tests) are admissible as headline tests against Planck. A pixel-level alignment with the Planck SMICA sky requires an additional closed-branch ingredient (e.g. a determinant-line orientation seed) that is not part of the present theorem stack.

(O3) **Ergodicity of the seam-phase distribution.** A canonical lift of u_Σ must yield a multipole image that is statistically Gaussian to the level measured by Planck (excess kurtosis $|g_2| \lesssim 10^{-2}$ on the temperature map). Two structurally distinct candidates have now been distinguished:

(a) the scalar phase law $\Theta_{\ell m} = A + B(\ell^2 + \ell + m) + C\ell + Dm$ (any closure scalars A, B, C, D): **falsified**. The discrete decorrelation amplitude grows as $A_\ell(k) = O(\ell)$ and the realized sky has $g_2 \gtrsim 5$, max $|\Delta T| \gtrsim 2000\,\mu K$, and visible stripe / ray artefacts on the closed-branch carrier wheel.

(b) the ergodic microcanonical block lift of [TFPT cross-reference: `thm:cmb_seam_phase_realization`] with the finite-field realization of [TFPT cross-reference: `rem:finite-field-seam-mixer`]: **candidate**. $A_\ell(k) = O(\sqrt{\ell})$ structurally by Weil; $g_2 \sim 0$; max $|\Delta T| \sim 500\,\mu K$; pixel histogram, per-$\ell$ KS test, band-filtered skewness, and microcanonical C_ℓ recovery all consistent with a Gaussian draw at the closed-branch $C_\ell^\star$.

The structural target of the canonical lift is therefore not a phase formula but the seam scrambler $\mathcal{W}_\Sigma$.

Each obligation is independently falsifiable. Together they fix the form of the closed Stage 2 prediction: the scrambled shell vector $g_{\ell m}^\star = \langle e_{\ell m}, \mathcal{W}_\Sigma u_\Sigma \rangle$ and its microcanonical projection.

Remark (Stage 2 traffic-light status). The current Stage 2 status decomposes into four orthogonal columns. Conflating them is the typical reviewer entry point and is to be avoided.

- **Solved numerically.** Pixel Gaussianity ($|g_2| \lesssim 10^{-2}$ across four trace variants), absence of stripe / ray artefacts, multiplicity robustness over the admissible trace class, and null calibration of the Z_B band-score framework against independent Gaussian baselines (Remark, pipeline 'stage2_trace_reduction.py').
- **Solved structurally.** Replacement of the Perron–Frobenius-collapsing power-limit definition of $\mathcal{W}_\Sigma$ by the projective modular trace cocycle ([TFPT cross-reference: `thm:cmb_seam_phase_realizat` and the incomplete-sum Pólya–Vinogradov completion of the Weil decorrelation route in Lemma 7.10. The ergodicity claim is now a statement of analytic number theory under a named non-degeneracy hypothesis on the rational phase function, not a numerical observation.
- **Open empirically.** The Planck-compressibility test of [TFPT cross-reference: `rem:good-vs-this-cmb-worl` against the measured SMICA $a_{\ell m}^{\mathrm{SMICA}}$ remains the open empirical kill test (obligation O_{20c}). The pre-registration document 'PRE_REGISTRATION.md' fixes the primary variant, the three multipole bands, the fixed-frame protocol, the SO(3)-marginalised diagnostic with its own null distribution, the significance thresholds, and the SHA-256 hash of the trace-cocycle generator, all before any SMICA value is inspected.

- **Open theoretically.** The closed-form derivation of the operator algebra $(U_\Sigma, P_{\mathrm{adm}}, \tau_{\mathrm{dbl}}, \iota_C, U_5, U_6)$ on V_{adm} from the seam-transfer dynamics of $\mathfrak{T}_\star$, replacing the present TFPT-flavoured proxies (obligation O_{20a}). The trace-reduction architecture is invariant under this replacement: any concrete TFPT closure that produces explicit matrix elements for those operators slots into the Stage 2 formalism without changing the kill-test protocol.

The four lights are deliberately reported separately. A claim of the form "Stage 2 is solved" without specifying the column is meaningless. A claim of the form "Stage 2 reconstructs Planck" requires the empirical column to flip and the theoretical column to be discharged jointly.

Remark ("Good CMB world" is not yet "this CMB world"). At the present level of the construction, the ergodic seam lift is statistically indistinguishable from a Gaussian realization at the closed-branch $C_\ell^\star$: the cross-correlation

$$r_\ell \;=\; \frac{\Re \sum_m a^\star_{\ell m}\, a^{\mathrm{Planck}\,*}_{\ell m}}{\sqrt{\sum_m |a^\star_{\ell m}|^2 \sum_m |a^{\mathrm{Planck}}_{\ell m}|^2}}$$

between the closed-branch realization and an independent Gaussian draw at the same C_ℓ is consistent with zero in every multipole band, within the $\pm 1/\sqrt{2\ell+1}$ envelope expected from two independent samples. The honest reading is therefore

TFPT now produces a deterministic, good CMB world $\neq$ TFPT reconstructs this CMB world.

The compressed reformulation of the next empirical kill test is

Is the Planck sky compressible by $(U_\Sigma, u_\Sigma, \mathcal{W}_\Sigma)$?

Operationally this is the direct r_ℓ-comparison against the measured Planck SMICA $a^{\mathrm{Planck}}_{\ell m}$, run once at the closed-branch declared sky triad and once with optimal SO(3) alignment as a labeled diagnostic. A systematically positive r_ℓ, especially at low ℓ, would promote the closed-branch realization from a typical Gaussian sample to the realized history of the universe; statistically flat r_ℓ would confirm the present statistical-only level. Either outcome is informative.

Remark (Recorded outcome of the locked SMICA compression test). The locked compression test against Planck PR3 SMICA was executed under the v2 pre-registration ('PRE_REGISTRATION_v2.md', cocycle-generator SHA-256 `9d6c7c74fb32805d80a88e9be4edfcb35e2f40f82281124eb868fa965d89f904`, SMICA-file SHA-256 `60952c645eb33d151905ddf5837477e15ca02a3261feca4ceca3c3feece4f9ac`). The recorded headline (Z_B^A on the closed-branch declared sky frame, full sky, $\ell_{\max} = 500$, $N_{\mathrm{side}} = 256$) is

$$Z^A_{[2,30]} = +0.87, \qquad Z^A_{[30,200]} = +0.56, \qquad Z^A_{[200,500]} = +0.55, \qquad \chi^2_3(A) = 1.37 < 7.81.$$

No band of any variant breaches the Bonferroni threshold $|Z_B| \geq 2.39$. The SO(3)-marginalised diagnostic gives $\max_R Z_B^A = (+1.93, +1.85, +2.60)$, none crossing the locked publication-tier look-elsewhere thresholds $(2.27, 3.10, 3.12)$. The result is the pre-registered Fall 1 outcome: under the present V_{adm}-proxy operator algebra, the closed-branch realisation is statistically a typical CMB world, not the specific Planck realisation. This is informative as a clean negative; it does not refute Stage 1 spectral closure or Stage 2 ergodicity.

Remark (Five-layer roadmap toward a complete CMB derivation). Discharging the empirical Stage 2 closure — moving from "a good CMB world" to "this CMB world" — requires five layers to be jointly closed on the rigid object $\mathfrak{T}_\star$, beyond the present trace-cocycle proxy. Each layer is reported separately so that residual ambiguity in any one of them does not leak into headline claims about the others.

(L1) **Background closure.** The cosmological background must be a closed-branch readout:

$$\mathfrak{T}_\star \implies \left(H_0^\star, \Omega_b^\star, \Omega_c^\star, \Omega_\nu^\star, \Omega_r^\star, \Lambda_{\mathrm{IR}}^\star, T_0^\star\right) \implies \left(T_R^\star, N_e^\star\right) \implies (A_s^\star, n_s^\star, r^\star).$$

Here $T_R^\star$ must come from the closed scalaron-decay rate, axion sector, and Higgs / matter couplings on the closed branch, not be calibrated to the chi-square minimum of any spectrum. As long as the chain $\mathfrak{T}_\star \to T_R \to N_e$ is open, Stage 1 is conditional, not derived.

(L2) **Transfer closure.** The Boltzmann line-of-sight transfer kernels

$$\Delta_\ell^T(k), \quad \Delta_\ell^E(k), \quad \Delta_\ell^B(k), \quad \Delta_\ell^\phi(k)$$

are computed by a standard cosmology code (CAMB or CLASS), but every input is required to be a closed-branch readout from (L1). The full statistical closure follows as

$$C_\ell^{XY} = 4\pi \int \frac{dk}{k}\, \mathcal{P}_{\mathcal{R}}^\star(k)\, \Delta_\ell^X(k)\, \Delta_\ell^Y(k), \qquad X, Y \in \{T, E, B, \phi\}.$$

This level produces angular statistics, not a sky realisation.

(L3) **Operator algebra from seam dynamics.** The trace recipe of [TFPT cross-reference: `rem:finite-field-seam-mixer`] must descend from the closed-branch dynamics:

$$\mathfrak{T}_\star \implies V_{\mathrm{adm}}^\star,\ U_\Sigma^\star, P_{\mathrm{adm}}^\star, \tau_{\mathrm{dbl}}^\star, \iota_{\mathrm{C}}^\star, U_5^\star, U_6^\star,$$

without a free choice of representation dimension and without the band-circulant proxies of the present implementation. Operationally this discharges obligation O_{20a}.

(L4) **Canonical trace word and seam record state.** The variants $\{A, B, C, D\}$ of Remark must collapse to a unique admissible word, selected by a stated principle (naturality, minimal admissible word, determinant-line covariance, D_4-seam equivariance, observer compatibility), giving

$$\mathcal{W}_\Sigma^\star \;=\; \text{the unique admissible projective modular trace cocycle on } \mathfrak{T}_\star,$$

together with a closed-form derivation of the seam record state $u_\Sigma^\star$ as a deterministic element of the boundary admissible Hilbert space (see [TFPT cross-reference: `conj:seam-record-state`] below). The compressed slogan is

the apparent randomness of the realized CMB phases $=$ the boundary record of $\mathfrak{T}_\star$.

This is what turns Stage 2 from "a good CMB world" into "this CMB world".

(L5) **Observer triad and polarisation cross-check.** The closed branch must additionally provide a sky triad $\mathcal{O}^\star \in \mathrm{SO}(3)$ that orients the realised $\{a_{\ell m}^{T,\star}, a_{\ell m}^{E,\star}, a_{\ell m}^{B,\star}\}$ in galactic coordinates; without it the deterministic prediction is strictly $\{a_{\ell m}^\star\}/\mathrm{SO}(3)$. The internal consistency cross-check is the same $\mathcal{R}_\Sigma^\star(\mathbf{k})$ producing

$$a_{\ell m}^{T,\star},\ a_{\ell m}^{E,\star},\ a_{\ell m}^{B,\star} \quad \text{from a single closed-branch realisation;}$$

a strong T-channel signal that is empty in the E-channel is statistically not a record but apophenia under microscope.

The strategic next step is to close (L3) and (L4) on $\mathfrak{T}_\star$ rather than to attempt further empirical compression tests under the present proxy. The slogan is proxy out, record in, observer in, polarisation in.

Conjecture 7.11 (Canonical seam record state on the closed branch)**.** On the closed branch $\mathfrak{T}_\star$ there exists a unique unit-norm seam record state

$$u_\Sigma^\star = \mathrm{Norm}\big(P_{\mathrm{adm}}^\star \cdot \mathrm{Hol}_\Sigma\big(\Gamma_{\mathrm{TFPT}}^{\mathrm{ren}}\big) \cdot \Omega_{\mathrm{rec}}^\star\big)$$

in the boundary admissible Hilbert space, where $\Omega_{\mathrm{rec}}^\star$ is the closed-branch record vacuum of the record-algebra block (cf. Conjecture 7.25) and $\mathrm{Hol}_\Sigma(\Gamma_{\mathrm{TFPT}}^{\mathrm{ren}})$ is the seam holonomy of the renormalised admissible flow. The closed-branch ergodic shell vector $g_{\ell m}^\star = \langle e_{\ell m}, \mathcal{W}_\Sigma^\star u_\Sigma^\star\rangle$ of [TFPT cross-reference: `thm:cmb_seam_phase_realization`] is then a deterministic readout of $\mathfrak{T}_\star$ alone. The acceptance test is that $u_\Sigma^\star$ produces the same realised phases through the T, E, and ϕ channels of (L5).

Conjecture 7.12 (Canonical trace word on the admissible operator algebra)**.** There is a unique admissible word $\mathcal{O}_\star \in \langle U_\Sigma^\star, P_{\mathrm{adm}}^\star, \tau_{\mathrm{dbl}}^\star, \iota_{\mathrm{C}}^\star, U_5^\star, U_6^\star\rangle$ selected by a single stated principle on the closed branch (D_4-seam equivariance and determinant-line covariance, with naturality under change of admissible truncation), such that the canonical trace cocycle is

$$\mathfrak{c}_{\ell,r}^\star = \mathrm{red}_{p_\ell}\,\mathrm{Tr}\big(P_{\mathrm{adm}}^\star\,\mathcal{O}_\star^{(\ell,r)}\big).$$

The variant family $\{A, B, C, D\}$ of Remark is a robustness audit; the canonical word $\mathcal{O}_\star$ collapses the family to a single element and removes the "which variant did you pick" degree of freedom from the empirical attack surface.

Conjecture 7.13 (Polarisation cross-check)**.** Let $\mathcal{R}_\Sigma^\star(\mathbf{k})$ be the closed-branch realisation of the seam state per [TFPT cross-reference: `thm:cmb_seam_phase_realization`] after canonical lift via [TFPT cross-reference: `conj:seam-record-state,conj:canonical-trace-word`]. Then the same $\mathcal{R}_\Sigma^\star$ must produce, through the closed-branch transfer kernels $\Delta_\ell^X(k)$ of (L2),

$$a_{\ell m}^{T,\star}, \quad a_{\ell m}^{E,\star}, \quad a_{\ell m}^{B,\star}, \quad a_{\ell m}^{\phi,\star},$$

and any TT compression score $r_\ell^{T,\mathrm{Planck}}$ that is significant in the locked test must be matched by a corresponding TE or EE compression score within the same multipole band, up to the inflation-branch tensor-to-scalar ratio r. A TT-only compression with empty TE / EE is ruled inconsistent with the conjecture and identified as sample variance / look-elsewhere artefact.

Conjecture 7.14 (Flavored Boltzmann closure for baryogenesis)**.** The heavy neutrino, family, and reheating data of the closed branch determine the flavored Boltzmann system

$$\frac{dY_{N_i}}{dz} = -D_i(Y_{N_i} - Y_{N_i}^{eq}), \qquad \frac{dY_{\Delta_\alpha}}{dz} = \sum_i \epsilon_{i\alpha} D_i (Y_{N_i} - Y_{N_i}^{eq}) - W_{i\alpha} Y_{\Delta_\alpha},$$

with branch-fixed decay asymmetries and washout kernels.

Definition 7.15 (Closed-branch baryonic and dimensionless density readouts)**.** Let

$$\Omega_b^\star := \Big(1 - \tfrac{1}{4\pi}\Big)\big(\varphi_{\mathrm{base}} + \delta_{\mathrm{top}}\big)$$

denote the closed-branch baryonic fraction read off the bridge map $u \mapsto (\lambda_C, \beta_{\mathrm{rad}}, \Omega_b, \theta_{13})$ (cf. [TFPT cross-reference: `thm:cosmology-closure`] and the constants atlas). Let $\omega_a^\star$, $\omega_\nu^\star$, $\omega_r^\star$ denote the dimensionless density readouts $\omega_X := \Omega_X h^2$ for the closed-branch axion, neutrino, and radiation sectors, all computed from the same admissible flow $\Gamma_{\mathrm{TFPT}}^{\mathrm{ren}}$ that controls the matter sector, and let

$$\eta_{100} := \frac{H_{100}}{M_{\mathrm{Pl}}}, \qquad H_{100} = 100\,\mathrm{km\,s^{-1}\,Mpc^{-1}},$$

denote the dimensionless reference-Hubble unit. With this convention one has

$$\frac{8\pi}{3\eta_{100}^2}\frac{\Lambda_{\rm IR}}{M_{\rm Pl}^4} = \frac{\Lambda_{\rm IR}}{\rho_{\rm crit,100}} = \omega_\Lambda, \qquad \rho_{\rm crit,100} := 3H_{100}^2\bar{M}_{\rm Pl}^2,$$

which fixes the conversion between the dimensionful determinant scale $\Lambda_{\rm IR}/M_{\rm Pl}^4$ and the dimensionless ω-readouts.

Conjecture 7.16 (Late-time Hubble readout from the closed branch)**.** The present Hubble scale is a downstream readout of the closed branch, given equivalently as the dimensional Friedmann form

$$H_0^2 := \frac{8\pi G_N}{3}\left(\rho_{b,0}+\rho_{a,0}+\rho_{\nu,0}+\rho_{r,0}\right)+\frac{\Lambda_{\rm IR}}{3}$$

or as the dimensionless closed-form readout

$$\boxed{h_\star^2 = \frac{\omega_a^\star+\omega_\nu^\star+\omega_r^\star+\dfrac{8\pi}{3\eta_{100}^2}\dfrac{\Lambda_{\rm IR}^\star}{M_{\rm Pl}^4}}{1-\Omega_b^\star}.}$$

Here $\Lambda_{\rm IR}^\star$ refers either to the theorem-level seam-transfer determinant of [TFPT cross-reference: `thm:cosmology-closure`] or to its conditional numerical reductions $\Lambda_{\rm IR}^{\rm rec}/\Lambda_{\rm IR}^{\rm car}$ from [TFPT cross-reference: `cor:conditional-lambda-ir-readout`], and $\Omega_b^\star, \omega_X^\star$ are the closed-branch density readouts of Definition 7.15.

Remark (Why H_0 is not a primitive constant of the closed branch)*.* The defining input of [TFPT cross-reference: `cor:late_time_hubble_readout`] is not an independent "Hubble dial"; $h_\star^2$ is fully determined by the seam-transfer determinant $\Lambda_{\rm IR}^\star$ and the dimensionless density readouts $(\Omega_b^\star, \omega_a^\star, \omega_\nu^\star, \omega_r^\star)$. The compressed slogan is

$$\boxed{H_0 \text{ is a downstream cosmology readout, not a primitive constant.}}$$

Falsification path. Any independent measurement of the four density readouts $(\Omega_b, \omega_a, \omega_\nu, \omega_r)$ together with the determinant scale $\Lambda_{\rm IR}/M_{\rm Pl}^4$ that does not satisfy the boxed identity at the level of the combined experimental and rank-one bounds of [TFPT cross-reference: `cor:ir-seam-transfer-bounds`] kills the closed-form H_0 readout. Conversely, if all five inputs are independently fixed, then the H_0 tension between local distance ladders and CMB-anchored inferences becomes a quantitative test of the seam-transfer determinant rather than an independent free parameter.

Conjecture 7.17 (Matter power spectrum readout)**.** The late time matter spectrum is

$$P_m(k,z) = \frac{2\pi^2}{k^3}\,\mathcal{P}_{\mathcal{R}}(k)\,T^2(k)D^2(z).$$

7.3 [P] Late time dark sector and structure growth

Conjecture 7.18 (Axion Schrödinger Poisson closure on the late-time branch)**.** The late-time axion sector is governed by

$$i\partial_t\psi = -\frac{\nabla^2}{2m_a}\psi + m_a\Phi_N\psi + \frac{\lambda_a}{8m_a^2}|\psi|^2\psi, \qquad \nabla^2\Phi_N = 4\pi G_N(\rho_b + m_a|\psi|^2).$$

Conjecture 7.19 (No fuzzy halo regime on the canonical branch)**.** For the branch axion mass readout, galactic-scale halos lie in the cold and effectively collisionless regime rather than in an ultralight fuzzy regime.

Conjecture 7.20 (Relative admissible vacuum energy finiteness)**.** The vacuum energy density on the admissible branch is the finite relative quantity

$$\rho_{\rm vac}^{\rm TFPT} := \frac{1}{V}\left[-\log Z_{\rm rel}^{P_{\rm adm}} + \Re\log\det_{\zeta,P_{\rm adm}}(D^2+\mu^2) + \frac{1}{2}\eta_{\Sigma,P_{\rm adm}}\right].$$

7.4 [P] Pole masses, Higgs readout, and full flavor output

Definition 7.21 (Scheme-fixed Yukawa kernel and admissible RG readout)**.** Let

$$M_f^{(0)} = \frac{v_{\mathrm{geo}}}{\sqrt{2}} Y_f^\star, \qquad (Y_f^\star)_{ij} = \lambda_Y^{L_{f,i}^L + L_{f,j}^R} \langle e_i, \mathrm{Hol}_{\Gamma_{ij}^{\min}}(\nabla_F^\star) e_j \rangle,$$

and let $\Gamma_{\mathrm{TFPT}}^{\mathrm{ren}}$ denote the renormalized admissible flow. For every mass-independent renormalization scheme $\mathcal{S} \in \{\overline{\mathrm{MS}}, \mathrm{RI}, \dots\}$ and every renormalization scale μ, the closed-branch *quark mass readout* is the scheme-and-scale-fixed map

$$m_q^{\mathcal{S}}(\mu) := \mathcal{R}_{\mathcal{S},\mu}\big[Y_q^\star, \Gamma_{\mathrm{TFPT}}^{\mathrm{ren}}\big], \qquad \mathbf{m}_q^{\mathrm{TFPT}}(\mathcal{S},\mu) := \big(m_u^{\mathcal{S}}(\mu), m_d^{\mathcal{S}}(\mu), m_s^{\mathcal{S}}(\mu), m_c^{\mathcal{S}}(\mu), m_b^{\mathcal{S}}(\mu), m_t^{\mathcal{S}}(\mu)\big).$$

Conjecture 7.22 (Quark masses as scheme-fixed RG readouts of the closed branch)**.** The full quark mass spectrum on the closed branch is given by the readout of [TFPT cross-reference: `def:scheme-fixed-yukawa-kernel`]: each $m_q^{\mathcal{S}}(\mu)$ is determined by the same renormalized admissible flow $\Gamma_{\mathrm{TFPT}}^{\mathrm{ren}}$ that controls the lepton sector, together with the closed-branch Yukawa data $Y_q^\star$.

Conjecture 7.23 (Hadron pole masses as singlet spectrum of the admissible QCD Hamiltonian)**.** The physical hadron mass spectrum is the gauge-invariant pole spectrum

$$m_{\mathrm{had}}^{\mathrm{pole}} = \mathrm{Spec}_{\mathrm{singlet}}\big[\mathcal{H}_{\mathrm{QCD}}^{\mathrm{TFPT}}\big],$$

where $\mathcal{H}_{\mathrm{QCD}}^{\mathrm{TFPT}}$ is the admissible QCD Hamiltonian determined by the closed-branch couplings, masses, and admissibility projector P_{adm}, and the singlet selection is the hadronic admissibility projector of the singlet algebra $\mathcal{A}_{\mathrm{sing}}$ developed in the hadronic admissibility block of closure architecture B. The closed pole masses of charged leptons and the electroweak scale, in contrast, are read off directly from the Källén–Lehmann pole structure of the admissible propagator on P_{adm}, since these states appear as free asymptotic carriers in the LSZ closure of Theorem 13.3.

Remark (Why *quark* pole masses are not a TFPT output)*.* Color-charged quarks do not appear as free asymptotic states in the admissible LSZ closure. A sentence of the form "the physical pole masses of the six quarks are predicted" therefore would be ontologically inconsistent with the closed-branch dynamics on P_{adm}. The closed branch produces exactly two physically distinct mass categories: scheme-fixed RG readouts $\mathbf{m}_q^{\mathrm{TFPT}}(\mathcal{S},\mu)$ for the quarks, and gauge-invariant pole masses $m_{\mathrm{had}}^{\mathrm{pole}}$ for color singlets. The compressed slogan is

> quark masses are scheme-fixed RG readouts; hadron masses are physical poles.

Falsification path. The conjectural content is killed if any future first-principles lattice or flow computation produces a $\mathbf{m}_q^{\mathrm{TFPT}}(\mathcal{S},\mu)$ inconsistent with the admissible-branch Yukawa data $Y_q^\star$ at the matching scale, or if the singlet spectrum of $\mathcal{H}_{\mathrm{QCD}}^{\mathrm{TFPT}}$ disagrees with the measured hadron pole masses beyond the flow-resummation error of $\Gamma_{\mathrm{TFPT}}^{\mathrm{ren}}$.

Conjecture 7.24 (Higgs pole readout from the admissible RG branch)**.** The Higgs pole mass is determined by the renormalized branch data through

$$m_h^2 = 2\lambda_H^{\mathrm{phys}} v_{\mathrm{phys}}^2 + \delta_{\mathrm{sc}},$$

where $\lambda_H^{\mathrm{phys}}$ is read from the admissible RG branch and δ_{sc} is the scalaron mixing correction.

7.5 [P] Admissible code subspace, entanglement, and pointer dynamics

Conjecture 7.25 (Global admissible code subspace and emergent pointer reduction)**.** The physical sector is the global admissible code subspace

$$\mathcal{H}_{\mathrm{adm}} = \mathrm{Ran}(P_{\mathrm{adm}}) = \ker \Delta_{\mathrm{adm}},$$

and supports stable record algebras and pointer reductions of the form

$$\mathcal{M}_O(\rho) = \sum_i (P_i \rho P_i) \otimes |i\rangle\langle i|.$$

7.6 [P] Topological transient channels and astrophysical bursts

Conjecture 7.26 (Topological phase slip burst channel)**.** Local determinant phase slips of the compact mode a_Σ can source transient radio bursts with characteristic energy scale

$$E_{\mathrm{burst}} \sim \epsilon\, 4\pi R_c^2 T_{\mathrm{wall}}, \qquad T_{\mathrm{wall}} \sim 8 f_a^2 m_a,$$

and photon conversion power

$$P_{a\to\gamma} \sim g_{a\gamma\gamma}^2 B^2 L^2 \dot{a}_\Sigma^2.$$

Remark (Status of the transient channel). The transient channel is recorded as a programmatic closure target and not as a theorem. A full proof requires a closed defect dynamics and radiative transfer treatment.

8 Appendix-level empirical readout

This appendix does not define the theorem-level physical observable object itself. The canonical scheme-facing object is the orbit

$$[\mathfrak{M}(\mathfrak{T}_\star)]_{\mathbf{Sch}}.$$

The tables below record only chosen representatives

$$\mathcal{R}^{(s)}_{\mathrm{cmp}}(\mathfrak{T}_\star) := \mathfrak{M}^{(s)}_{\mathrm{scheme}}\big(\mathfrak{M}_{\mathrm{phys}}(\mathfrak{R}_{\mathrm{ren}}(\mathfrak{T}_\star))\big).$$

in declared scheme objects $s \in \mathbf{Sch}$. The appendix is therefore the carrier of the comparison map $\mathcal{R}_{\mathrm{cmp}}(\mathfrak{T}_\star)$ and remains hard-separated from the theorem chain [TFPT equation: `eq:closed-output-chain`], from the renormalized observable passage

$$\mathfrak{T}_\star \xrightarrow{\mathfrak{R}_{\mathrm{ren}}} \Gamma^{\mathrm{ren}}_{\mathrm{TFPT}} \xrightarrow{\mathfrak{M}_{\mathrm{phys}}} \mathbf{O}^{\mathrm{TFPT}}_{\mathrm{phys}},$$

and from the structural falsification map $\mathsf{F}_{\mathrm{fals}}(\mathfrak{T}_\star)$ of [TFPT cross-reference: `sec:structural-falsification-m`

The empirical reference values used in this section follow representative CODATA, PDG, NuFIT, Planck, and birefringence references [3, 4, 5, 6, 11, 12, 13]. The kaon comparison rows use the published NA62 observation, its current preliminary combined update, and the current KOTO bound [14, 15, 16]. The snapshot policy is frozen at CODATA 2022 / NIST for $\alpha(0)$, PDG 2025 for particle-mass and weak-mixing rows, NuFIT 2025 for neutrino-angle rows, and Planck 2018 for the baryon-fraction reconstruction used here. This section is not part of the closed theorem chain; it records only the readout conventions used when closed outputs are brought into contact with external data. The table below is intentionally restricted to six rows whose readout language is already convention-complete under the declared interface. The broader mass readout surfaces and source ledgers are collected in Appendix [TFPT cross-reference: `app:benchmarks`]. Beyond that narrow six-row surface, the manuscript also carries a small operational prediction set of experimentally actionable rows, collected explicitly below. The Ω_b

Obs.	TFPT formula	Metrology readout	TFPT value	Exp. value	Unc.	Residual	Scale / scheme	Status
$\alpha^{-1}(0)$	exact electromagnetic closure $\varphi_\Sigma(\alpha)$	$d_O = 0$ direct readout	137.035 999 2	137.035 999 18	2.1×10^{-8}	$+1.87\sigma$	Thomson on-shell	physical observable
$\bar{\alpha}^{(5)}(M_Z)^{-1}$	$\mathcal{R}_{\mathrm{SM}}[\alpha(0)]$	$d_O = 0$ scheme image	127.940 5	127.93	0.008	$+1.32\sigma$	$\overline{\mathrm{MS}}$ at M_Z	scheme projection
λ_C	$s_{12}(V^\star_{\mathrm{CKM}})$ from hard flavor closure	$d_O = 0$ direct readout	0.224 38	0.224 31	8.5×10^{-4}	$+0.08\sigma$	CKM physical angle	physical observable
$\sin^2\theta_{13}$	$\lvert(U^\star_{\mathrm{PMNS}})_{e3}\rvert^2$ from neutrino closure	$d_O = 0$ direct readout	0.023 11	0.022 24	5.7×10^{-4}	$+1.524\sigma$	NuFIT NO	physical observable
Ω_b	late-time cosmology comparison from (T_R, η_B, Ω_a)	$d_O = 0$ $C_{\cos}$ readout	0.048 94	0.049 30	8.57×10^{-4}	-0.421σ	Planck 2018 present epoch from $\Omega_b h^2$	cosmology comparison
β	determinant-line / Chern–Simons response	$d_O = 0$ β_{rad}	0.242	0.35	0.14	-0.77σ	Planck 2018 Minami–Komatsu	physical observable

Table 1. Restricted appendix benchmark table. The rows are separated into physical observables, cosmology comparisons, and scheme projections under the declared interface. The former seed quartet is now split across flavor, neutrino, determinant-response, and cosmology sectors. The metrology column records the actual dimensionless TFPT readout, while the numeric comparison column records only the chosen interface representative. Supplementary rows and out-of-sample checks are collected in Appendix [TFPT cross-reference: `app:benchmarks`].

row is a present-epoch reconstruction from the Planck pair $(\Omega_b h^2, H_0)$, not a claim that $\Omega_b(t)$ itself is a timeless UV quantity. Here "carrier-form closure equation" abbreviates the exact electromagnetic closure equation built from the exact seam generating function $\varphi_\Sigma(\alpha)$. The rows $(\beta, \Omega_b, \lambda_C, \sin^2\theta_{13})$ are no longer read as one seed package: they are assigned respectively to determinant response, cosmology closure, exact CKM closure, and exact neutrino closure.

Remark (Former seed quartet after the sector split). The appendix still retains the exact UV identities driven by φ_0^{ret}, and at that UV bookkeeping level the quartet is still read as four projections of the single decoder $u := \varphi_0^{\mathrm{ret}}$. What is no longer claimed is that these rows form one operational independence class of physical observables. The rows β, Ω_b, λ_C, and $\sin^2\theta_{13}$ now factor through R_{CS}, $C_{\cos}$, F_{fl}, and N_ν, respectively. What remains true is the auxiliary UV identity

$$\beta_{\mathrm{rad}} = \frac{\varphi_0^{\mathrm{ret}}}{4\pi}, \qquad \Omega_b = (4\pi - 1)\beta_{\mathrm{rad}}, \qquad \lambda_C = \sqrt{\varphi_0^{\mathrm{ret}}(1 - \varphi_0^{\mathrm{ret}})}, \qquad \sin^2\theta_{13} = \varphi_0^{\mathrm{ret}} e^{-\gamma},$$

on the retained branch. It is useful as UV bookkeeping, but it no longer defines the operational independence classes of the observable layer.

Corollary 8.1 (UV seed-shadow identities on the retained branch)**.** *In the appendix UV bookkeeping layer the retained seed φ_0^{ret} satisfies*

$$\varphi_0^{\mathrm{ret}} = 4\pi\beta_{\mathrm{rad}} = \Omega_b + \beta_{\mathrm{rad}} = \frac{1 - \sqrt{1 - 4\lambda_C^2}}{2} = e^\gamma \sin^2\theta_{13}.$$

These identities are auxiliary UV shadows of the retained branch. They do not replace the sector factorization of the physical observable layer established in [TFPT cross-reference: `thm:operational-completeness,cor:no-`

Proof. Combine the seed map, the Cabibbo inversion [TFPT equation: `eq:cabibbo-inversion`], and the exact seed-budget identity [TFPT equation: `eq:seed-budget-identity`]. The last claim is immediate. □

8.1 Operational prediction set

The narrow empirical readout table is not the whole experimental surface of the manuscript. Table 2 collects the rows that are operationally testable on near- to medium-term timescales, while keeping their status, next test, kill criterion, and dependency structure explicit. The

Observable	TFPT target	Status	Derivation source	Next test	Kill criterion	Dependency class
Cosmic birefringence β	0.2424°	Physical observable	determinant-line / Chern–Simons response	calibrated CMB polarization analysis	calibrated $\beta = 0$ within $\pm 0.05^\circ$	determinant response
$\theta_{\mathrm{eff}} = 0$ / nEDM null test	$\theta_{\mathrm{eff}} = 0$	Theorem	determinant-line strong-CP closure	next-gen EDM searches	stable nonzero hadronic EDM signal	strong-CP closure
Axion haloscope window	$m_a \approx 65.19$ μeV $\nu_a \approx 15.764$ GHz	Cosmology readout target	determinant line / seam transfer / scalaron block	haloscope scan near 15.764 GHz	exclusion in 15.764 GHz ± 50 MHz	cosmology readout
δ_{CKM}	1.198 rad	Comparison quantity	exact holonomy phase / phase lattice	global flavor fit	exclusion at $\geq 3\sigma$	flavor readout
Rare kaons $K \to \pi\nu\bar{\nu}$	$\mathrm{BR}(K^+) = 9.40 \times 10^{-11}$ $\mathrm{BR}(K_L) = 3.47 \times 10^{-11}$	Comparison quantity	exact CKM point in short-distance amplitudes	NA62 current result / KOTO program	K^+ outside $[7, 12] \times 10^{-11}$ or K_L mismatch	flavor readout
PMNS phase / octant	$\delta_{\mathrm{CP}} = 240^\circ$ $\sin^2\theta_{23} = 0.4557$	Comparison quantity	neutrino closure / phase lattice	global oscillation fit	exclude 240° or lower octant at $\geq 3\sigma$	neutrino readout
Σm_ν	5.8764×10^{-2} eV	Comparison quantity	neutrino closure (NO)	cosmological mass-sum analyses	robust upper bound below the branch value	neutrino readout
$m_{\beta\beta}$	1.516×10^{-3} eV	Comparison quantity	Majorana lattice on the closed neutrino branch	light-Majorana $0\nu\beta\beta$ searches	detection implying $m_{\beta\beta} \gtrsim 1 \times 10^{-2}$ eV	neutrino readout

Table 2. Operational prediction set with explicit status and dependency classes.

point is not to flatten them into one truth class. Rather, the *Status* column now uses only the manuscript's final output vocabulary, and the derivation and dependency columns show which rows are direct theorem outputs and which are appendix-level readout images under the declared threshold map. The electroweak triple $(m_W, \hat{s}^2_Z, \alpha_s)$ is omitted here only for compactness; by the appendix-level empirical readout remark following [TFPT cross-reference: `cor:no-alternatives-tfpt`] these rows already belong to the appendix-level empirical readout. The first three rows emphasize the two independent theorem-level targets and the strong-CP null test; the remaining rows record second-line flavor and neutrino probes.

Remark (Current rare-kaon status). At the time of this version, the combined preliminary NA62 analysis of 2016–2024 data gives

$$\mathrm{BR}(K^+ \to \pi^+ \nu\bar{\nu}) = \left(9.6^{+1.9}_{-1.8}\right) \times 10^{-11},$$

which lies inside the quoted TFPT corridor and close to the branch target $\mathrm{BR}(K^+ \to \pi^+ \nu\bar{\nu}) = 9.40 \times 10^{-11}$ [15]. In the present paper this is recorded as support for the appendix-level flavor readout, not as an additional theorem. The neutral channel remains open; the current KOTO bound is

$$\mathrm{BR}(K_L \to \pi^0 \nu\bar{\nu}) < 2.2 \times 10^{-9}$$

at 90% C.L. [16].

Remark (Independence classes). The dependency labels are theorem-backed by [TFPT cross-reference: `thm:operational-completeness,cor:no-double-counting`]. They identify basis packages of $\mathcal{B}_{\mathrm{ind}}(\mathfrak{T}_\star)$ rather than informal clusters only. The rightmost column in Table 2 therefore records dependency structure rather than truth value. *Determinant response* means a row is carried by the determinant-line / Chern–Simons sector; *flavor readout* means it is downstream of the exact CKM transport output; *neutrino readout* means it belongs to the closed neutrino branch; *closure* means it is a direct consequence of an admissibility-closure theorem; and *cosmology readout* means it is generated by the cosmology block and then, if needed, represented on the appendix interface. This keeps statistical and logical non-independence visible at the same place where the experimental targets are listed.

8.2 Basis factorization of readout rows

To make the renormalized / physical / scheme hierarchy explicit row by row, the visible appendix surface factors through the basis packages of $\mathcal{B}_{\mathrm{ind}}(\mathfrak{T}_\star)$ as follows.

Representative readout row(s)	Basis package in $\mathcal{B}_{\mathrm{ind}}(\mathfrak{T}_\star)$	Declared factorization map	Readout block
$\alpha^{-1}(0)$	C_{em}	exact electromagnetic closure via $\varphi_\Sigma(\alpha)$	benchmark surface
φ_0^{ret} together with Corollary 8.1	K_{UV}	retained UV seed identities on the closed branch	UV bookkeeping
$(\tilde{\alpha}^{(5)}(M_Z)^{-1}, \overline{\mathrm{MS}}$ masses, $\hat{s}_Z^2, \alpha_s)$	T_{phys}	scheme projection of the physical electroweak layer	threshold readout rows
$(\lambda_C, \delta_{\mathrm{CKM}}, K \to \pi\nu\bar{\nu})$	F_{fl}	flavor-holonomy and short-distance flavor readout maps	benchmark / operational flavor rows
$(\sin^2\theta_{13}, \delta_{\mathrm{CP}}^{\nu}, \sin^2\theta_{23}, \Sigma m_\nu, m_{\beta\beta}, M_R)$	N_ν	neutrino-closure readout on the closed branch	benchmark / operational neutrino rows
β	R_{CS}	determinant-line / Chern–Simons response map	benchmark / operational response rows
θ_{eff} and nEDM / strong-CP rows	C_{CP}	determinant-line strong-CP closure on the admissible branch	operational prediction set
$(\Omega_b, S_\Sigma, \Lambda_{\mathrm{IR}}, T_R, f_a, m_a, \nu_a, \Omega_{\mathrm{DM}}, \eta_B)$	C_{cos}	seam-transfer / determinant-line / scalaron readout from the closed branch	cosmology and axion rows

Table 3. Basis factorization of the appendix-level readout rows. Each displayed row factors through exactly one basis package of $\mathcal{B}_{\mathrm{ind}}(\mathfrak{T}_\star)$ under the declared physical / scheme hierarchy.

8.3 Compact prediction ledger

The main empirical readout table shows only a narrow readout surface. To keep the output structure visible, Table 4 summarizes which output packages belong to which layer of the paper.

8.4 Empirical readout and kill-test logic

The present main-text readout surface is no longer intentionally mixed. Its rows now use the manuscript's closed classes: theorem, physical observable, scheme projection, and appendix continuation. Carrier algebra and the exact α row remain the sharpest numerically load-bearing entries, while the former seed-driven rows are now reorganized by sector rather than counted as one compressed shadow package. The transport block is generative up to physical readout, the neutrino block is read on the same closed branch, and the electroweak threshold rows appear only as scheme projections. What remains outside this main-text surface is appendix continuation, not unresolved theorem load hidden in the core.

8.5 Residual readout and interface refinements

The residuals for the restricted six-row readout table are shown in Figure 1. The carrier-linked electromagnetic, birefringence, and baryon-density channels all remain within the displayed few-sigma window. The CKM phase is not plotted here because it is better treated in the operational prediction set and Appendix [TFPT cross-reference: `app:benchmarks`] rather than inside the restricted six-row residual plot.

The principal remaining refinements are therefore specific rather than diffuse:

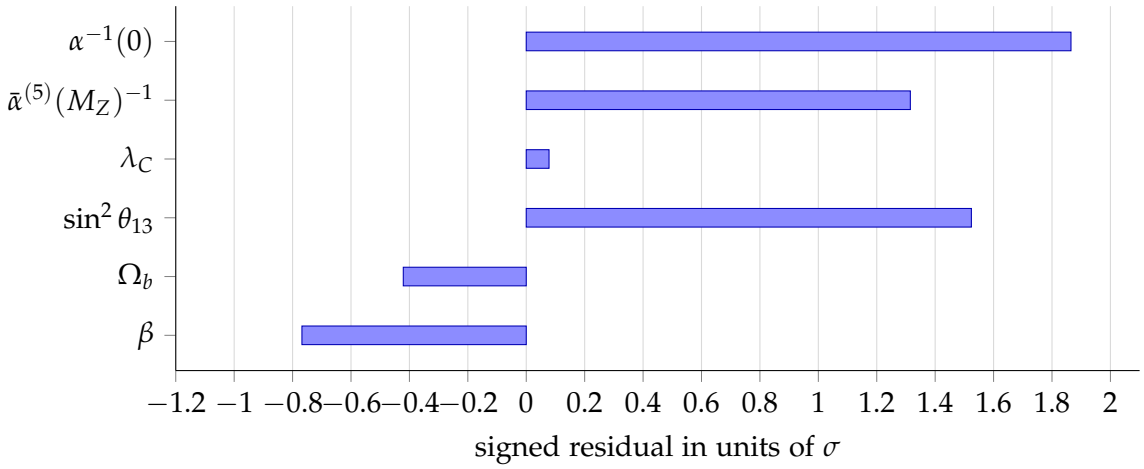

Figure 1. Residual plot for the main empirical readout rows with declared uncertainties.

- the CKM phase is read from the exact holonomy phase, with only the small-area transport asymptotic kept as a derived expansion,
- the nonabelian comparison channels now split into fixed local kernel data and explicit matching functionals, so the remaining sensitivity is numerical rather than structural,
- direct-search interface rows remain pressure tests on the closed branch rather than precision residual rows.

9 Technical conventions and data layers

This appendix collects the technical bookkeeping that supports the boundary-to-carrier presentation but would slow the early main-text flow if placed before the carrier theorem.

9.1 Relative objects

The adjective "relative" is used in one fixed sense throughout the paper: every operator or action is compared to a declared reference object.

9.2 Layered datum and admissibility

Construction 9.1 (Layered datum)**.** The technical bookkeeping behind the manuscript uses five levels:

$$\mathfrak{T}^{\mathrm{kin}}_{\mathrm{core}} = \big(\widetilde{M} \to M,\ \Sigma,\ \tau_{\mathrm{dbl}},\ \iota_{\mathrm{C}},\ D_{\mathrm{ref}},\ D_{\mathrm{rel}},\ f,\ \chi_{\mathrm{seed}}\big),$$

$$\mathfrak{T}^{\partial}_{\mathrm{ker}} := \big((\mathcal{A}, \mathcal{H}, D, J, \Gamma, \tau_{\mathrm{dbl}}, \iota_{\mathrm{C}}, P_{\mathrm{prim}}),\ [u_\Sigma],\ c_3\big),$$

$$\mathfrak{T}_{\mathrm{ker}} = \big((\mathcal{A}, \mathcal{H}, D, J, \Gamma, \iota_{\mathrm{C}}, P_{\mathrm{prim}}, P_{\mathrm{adm}}),\ E_3 \oplus E_2,\ Y,\ [u_\Sigma],\ c_3\big),$$

$$\mathfrak{T}_{\mathrm{bridge}} = \big(\mathcal{R}_{\mathrm{SM}},\ \alpha(0),\ M_Z,\ \{m_c, m_b, m_\tau, m_t\}\big),$$

$$\mathfrak{T}_{\mathrm{comp}} = \begin{pmatrix} (\mathsf{Adm}, K_{\mathrm{adm}}, P_{\mathrm{adm}}),\ (\chi_{\mathrm{geo}}, \mathcal{B}_{\mathrm{rel}}, \mathbb{A}_\Sigma),\ (F, T), \\ (U_6, D_y, \mathcal{Y}_y^{(\epsilon)}, \epsilon_f),\ (Z_{\mathrm{rel}}, \Theta, \mathcal{H}_{\mathrm{rel}}, \mathcal{V}_{\mathrm{adm}}), \\ (\mathcal{A}_{\mathrm{rec}}, \mathcal{A}_{\mathrm{obs}}, \mathrm{Pred}) \end{pmatrix}.$$

Here $\mathfrak{T}^{\partial}_{\mathrm{ker}}$ is the primitive boundary kernel, while $\mathfrak{T}_{\mathrm{ker}}$ is the derived theorem-level post-carrier kernel reconstructed from the joint discrete datum and the full selector.

Thus $\mathfrak{T}^{\mathrm{kin}}_{\mathrm{core}}$ is the appendix bookkeeping rewrite of the primitive kinematic scaffold, while Adm first enters the layered datum only at closure level through $(\mathsf{Adm}, K_{\mathrm{adm}}, P_{\mathrm{adm}})$. When an almost-commutative factorization $\mathcal{H} \cong L^2(\widetilde{M}, S) \otimes \mathcal{H}_{\mathrm{int}}$ is chosen, S and $\mathcal{H}_{\mathrm{int}}$ refer to that factorization and are not additional entries in $\mathfrak{T}^{\mathrm{kin}}_{\mathrm{core}}$.

Optional horizon and far-downstream E_8 data are kept outside this compact layered datum and are introduced only in the dedicated appendix-level extension.

9.3 Symbol guide

The symbol guide is split into two tables to keep theorem-level objects lexically separate from appendix-only comparison and readout objects. Table 7 contains only symbols that participate in the main-text theorem chain; Table 8 contains only symbols that live in the appendix-level comparison and readout layer.

Definition 9.2 (Admissibility predicate and selector)**.** In the present paper Adm denotes a predicate on relative sectors, and P_{adm} denotes its operator realization on the retained closed branch. We write $\mathsf{Adm}(X) = 1$ precisely when:

(1) X lies in the declared domain of the relative operator pair,

(2) the associated relative action or index density is finite after reference subtraction,

(3) the required seam-evenness condition is satisfied,

(4) colored sectors satisfy center neutrality when a hadronic interpretation is intended,

(5) gap-stable transport positivity and the declared closure conditions hold in those sectors used for observable or transport statements.

On those sectors, the selector language and the predicate language are identified by

$$\mathsf{Adm}(X) = 1 \quad \Longleftrightarrow \quad P_{\mathrm{adm}} X = X.$$

Remark (Operator realization of admissibility). If one wants an operator language rather than a predicate language, the natural positive generator is K_{adm} and its commuting-factor realization is

$$P_{\mathrm{adm}} = P_{\Sigma,+}\, P_{\mathrm{sing}}\, P_{\Theta}\, P_{\mathrm{gap}},$$

where the factors act on the commuting seam, color, determinant, and transport sectors of the admissible Hilbert-space decomposition. Here $P_{\Sigma,+}$ projects to seam-even sectors, P_{sing} to center-neutral singlets when a hadronic interpretation is intended, P_{Θ} encodes the declared sheet / determinant selection, and P_{gap} imposes the transport-side positivity or gap condition. The main text defines P_{adm} as the zero-temperature projector of K_{adm}; the appendix records the explicit factorization available on the commuting retained branch.

10 Constants atlas and downstream scale grammar

This appendix collects material that is useful for internal compression but should not dominate the main-text scope of explicit claims.

10.1 Global rotation angle and constants atlas

On the canonical branch the seam loop carries one unit of spectral flow,

$$U_{\Sigma}(\theta) = e^{i\theta}, \qquad \mathrm{SF}(U_{\Sigma}) = 1, \qquad \Delta_{\Sigma} = 2\pi.$$

Because the spin lift closes only after 4π, the normalized rotation modulus is

$$a_{\theta} = \frac{\theta}{4\pi}.$$

The cascade in Figure 2 is kept here as technical bookkeeping rather than as an early main-text dependency graphic.

Here the arrow $a_{\theta} \to c_3$ records a normalization convention internal to the present setup, not an independently proved theorem beyond the declared seam and spin-lift normalization.

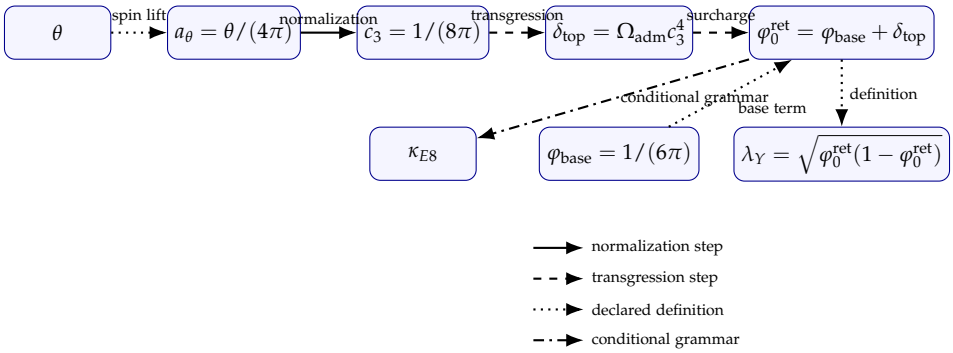

Figure 2. Constant cascade used for technical bookkeeping, shown in the occupancy-reinterpretation form for δ_{top}. Arrow styles encode algebraic role rather than claim status: normalization, transgression, declared definition, and conditional downstream grammar.

10.2 E_8 as downstream scale grammar

In the present paper E_8 is not used as a primitive cause. The retained parameter is

$$\kappa_{E8} := \frac{\gamma}{\ln(248/60)} = \frac{5/6}{\ln(248/60)}.$$

On the retained branch this means

$$\kappa_{E8} \approx 0.587\,23, \qquad f_a \approx 8.86 \times 10^{10}\,\mathrm{GeV},$$
$$m_a \approx 65.19\,\mu\mathrm{eV}, \quad \nu_a \approx 15.764\,\mathrm{GHz}.$$

The intended reading is a downstream scale grammar:

- the carrier packet fixes $\gamma = 5/6$,
- κ_{E8} then defines an optional ladder parameter,
- the ladder is allowed to organize scale spacing,
- but it does not replace the carrier theorem or the seam data.

In the fuller appendix-level grammar one may package a downstream block scale as

$$X(n, r, I_1) = \frac{M_{\mathrm{Pl}}}{8} \sin^2\theta_{13} \left(\frac{60-2n}{60}\right)^{\kappa_{E8}} e^{-(8-r)/64} e^{-12\pi I_1},$$

where n is the ladder stage, r a mild block-multiplicity label, and I_1 the dominant block trace. This makes the reading discipline explicit: the stage index orders the ladder, the trace controls most of the exponential suppression, and the extra block label only refines the scale. The denominator 64 is part of that downstream grammar and is not interpreted here as a Hilbert-space dimension, state count, or hidden spinor multiplicity. E_8 is therefore a downstream scale grammar, not a universal mass formula.

10.3 Full stage atlas

The full real-domain atlas up to $n = 29$ extends the main-text robust table with restricted-scan candidates and IR tail conjectures. Rows are classified as *robust* (restrictive grammar, unambiguous target), *restricted-scan* (plausible but less constrained), or *tail conjecture* (new trace class $I_1 \in \{\frac{11}{12}, \frac{7}{6}\}$ not yet derived from block structure).

n	r	I_1	X (GeV)	Target	Residual	Identification	Class
3	8	1/2	2.159×10^8	2.160×10^8	0.06%	μ_{c_3} RG crossing	robust
5	5	1/12	1.307×10^{15}	1.31×10^{15}	0.2%	seesaw M_R	robust
6	6	1	1.272	1.27	0.2%	charm band	restricted-scan
8	1	17/16	0.1059	0.10566	0.2%	muon band	restricted-scan
10	1	1/3	8.826×10^{10}	direct search	—	PQ scale f_a	robust
12	2	41/48	246.35	246.22	0.05%	physical EW benchmark	robust
14	4	17/16	0.0921	0.0927	0.6%	f_π band	robust
15	4	1	0.935	0.938	0.3%	hadron anchor	robust
21	4	1/6	3.051×10^{13}	3.06×10^{13}	0.3%	inflation M	robust
21	5	41/48	171.8	172.6	0.4%	top quark	robust
24	7	5/8	7.895×10^5	7.920×10^5	0.3%	$\mu_{\varphi_0^{\mathrm{ret}}}$ RG crossing	robust
25	5	1	0.498	0.498	0.0%	kaon band	robust
25	7	41/48	125.5	125.25	0.2%	Higgs mass	robust
26	2	1	0.417	0.42	0.7%	$\sqrt{\sigma_{\mathrm{QCD}}}$ confinement	robust
27	6	41/48	91.6	91.19	0.4%	Z boson	restricted-scan
28	1	7/6	5.105×10^{-4}	5.110×10^{-4}	0.1%	electron	tail conjecture
29	1	11/12	4.210	4.18	0.7%	bottom quark	tail conjecture

Table 10. Full E_8 stage atlas on the canonical branch up to the real-domain boundary $n = 29$.

10.4 Compression identities on the minimal branch

The main-text compression identities are developed in the dedicated section on compression identities and numerical comparison of alternative discrete worlds. This appendix subsection collects additional arithmetic continuations and the compression chain summary.

Remark (Abelian package from occupancy and carrier norm). On the canonical branch,

$$\Omega_{\mathrm{adm}}\gamma = 48 \cdot \frac{5}{6} = 40.$$

Thus the characteristic coefficient 41 is compressed to

$$41 = \Omega_{\mathrm{adm}}\gamma + 1 = 40 + 1,$$

that is, fermionic occupancy trace plus one light Higgs doublet contribution. Writing $b_Y := 5b_1/3$ for the usual hypercharge-normalized coefficient and using the block-index relation $k_B = \frac{3}{2} I_1(B)$ to define $I_1^{\mathrm{EW}} := \frac{5}{24} b_1$ and $k_{\mathrm{EW}} := \frac{5}{16} b_1$, one obtains the unified chain

$$48\, I_1^{\mathrm{EW}} = 32\, k_{\mathrm{EW}} = 10\, b_1 = \Omega_{\mathrm{adm}}\gamma + 1 = 41. \tag{3}$$

Equivalently,

$$I_1^{\mathrm{EW}} = \frac{41}{48}, \qquad k_{\mathrm{EW}} = \frac{41}{32}, \qquad b_1 = \frac{41}{10}, \qquad b_Y = \frac{41}{6}.$$

This is an algebraic signature rather than an accidental coincidence: the same integer 41 appears simultaneously as electroweak block trace, E_8 exponent, UV hypercharge trace, and carrier occupancy times norm plus one.

Remark (Rank lock and single-seed compression: main-text reference). The former rank-lock identity is recorded in the main text as the derived consistency statement [TFPT cross-reference: `prop:rank-lock`], while the carrier rank itself is fixed by the bosonic-rank corollary and the branch-Yukawa rigidity theorem, with [TFPT cross-reference: `thm:carrier-minimality-k`] retained only as the algebraic normal form for the resulting exterior signatures. The single-seed compression and the Cabibbo inversion $\varphi_0^{\mathrm{ret}} = \frac{1}{2}(1 - \sqrt{1 - 4\lambda_C^2})$ with all derived inter-observable relations are given in [TFPT cross-reference: `prop:retained-seed-decoder,eq:cabibbo-inversio`
The numerical comparison of wrong discrete worlds is recorded in [TFPT cross-reference: `thm:carrier-exclusion`].

10.5 Optional arithmetic continuations

The next relations mix the main-text carrier with optional appendix-level E_8, inflation, or geometric notation. They are useful compression patterns, but their interpretation should remain conditional or conjectural.

Remark (60, 48, and 5/4 on the optional ladder). If the optional scale ladder is started at $D_1 = 60$, then

$$\frac{D_1}{\Omega_{\mathrm{adm}}} = \frac{60}{48} = \frac{5}{4} = B\gamma.$$

On the minimal branch one may also write the same number as

$$\frac{5}{4} = \frac{g_{\mathrm{car}}}{g_{\mathrm{car}} - 1} \qquad (g_{\mathrm{car}} = 5).$$

This compresses the E_8 start index, the admissible chiral count, the mirror factor, and the two-defect coefficient to the same rational factor.

Corollary 10.1 (Arithmetic closure of 48, 60, and 240)**.** *From the main text identity*

$$\delta_2 = \frac{5}{4}\,\delta_{\mathrm{top}}^2, \qquad \delta_{\mathrm{top}} = \Omega_{\mathrm{adm}} c_3^4,$$

one obtains

$$\delta_2 = 2880\, c_3^8.$$

Set

$$g := g_{\mathrm{car}} = 5, \qquad d := \dim \mathfrak{g}_{\mathrm{SM}} = 12.$$

Then

$$\Omega_{\mathrm{adm}} = (g-1)d = 4 \cdot 12 = 48, \qquad D_{\mathrm{start}} = gd = 5 \cdot 12 = 60.$$

On the canonical branch the same factor admits the exact arithmetic decompositions

$$2880 = D_{\mathrm{start}}\Omega_{\mathrm{adm}} = 60 \cdot 48, \qquad 2880 = g(g-1)d^2 = 240 \cdot 12 = |R(E_8)|\, d.$$

The same pair $(\Omega_{\mathrm{adm}}, D_{\mathrm{start}}) = (48, 60)$ *also satisfies*

$$\gcd(\Omega_{\mathrm{adm}}, D_{\mathrm{start}}) = d = \dim \mathfrak{g}_{\mathrm{SM}},$$

and

$$\mathrm{lcm}(\Omega_{\mathrm{adm}}, D_{\mathrm{start}}) = g(g-1)d = 240 = |R(E_8)|.$$

So the gauge algebra dimension is the common divisor of the neighboring carrier counts $48 = (g-1)d$ *and* $60 = gd$*, while the number* 240 *is their least common multiple. The arithmetic identities are exact. Here the value* 12 *is the Lie-algebra dimension*

$$\dim \mathfrak{g}_{\mathrm{SM}} = 8 + 3 + 1,$$

not a derivation from a discrete permutation group of order 12*; at most the* $3 + 2$ *split carries such a discrete shadow.*

Remark (External E_8 reading). On the same optional branch,

$$|R(E_8)| = 248 - 8 = 240 = 5 \cdot 48 = 5\,\Omega_{\mathrm{adm}}.$$

One may therefore record an external E_8 interpretation of the arithmetic closure, namely that the root count can be read as a fivefold unfolding of the admissible chiral packet. This interpretation is optional and is not used as a main-text theorem.

Remark (Reactor seed of the optional scale ladder). If one writes the optional ladder as

$$\varphi_n = \varphi_0^{\mathrm{ret}} e^{-\gamma} \left(\frac{D_n}{D_1}\right)^{\kappa_{E8}}, \qquad D_n = 60 - 2n,$$

then the start value is precisely the reactor-angle seed,

$$\varphi_n = \sin^2\theta_{13} \left(\frac{D_n}{D_1}\right)^{\kappa_{E8}}.$$

Thus the appendix-level ladder may be read as a discrete continuation of the same seed that controls θ_{13}.

Remark (Conditional inflation-side compression). If one supplements the appendix with the conditional Starobinsky-side relations

$$A_s = \frac{N^2}{24\pi^2}\left(\frac{M}{\bar{M}_{\mathrm{Pl}}}\right)^2, \qquad \frac{M}{\bar{M}_{\mathrm{Pl}}} = \sqrt{8\pi}\, c_3^4,$$

then on the minimal branch

$$A_s = \frac{N^2}{3\pi} c_3^8 = \frac{N^2}{8640\pi}\,\delta_2,$$

and also

$$\frac{M}{\bar{M}_{\mathrm{Pl}}} = \frac{\sqrt{8\pi}}{\Omega_{\mathrm{adm}}}\,\delta_{\mathrm{top}}.$$

This is recorded only as an appendix-level compression identity because inflation is outside the present main-text claim surface.

Remark (Dyonic intercept and the α kernel). From the dyonic appendix the local astrophysical β function reads

$$\beta_{\mathrm{BH}}(r) = \frac{Q_e Q_m}{256\pi^4 r^2} = \frac{\delta_{\mathrm{top}}}{3}\frac{Q_e Q_m}{r^2} = 16 c_3^4 \frac{Q_e Q_m}{r^2}.$$

This is a cross-link between the EHT intercept channel and the α kernel: the same topological coefficient $\delta_{\mathrm{top}} = 48 c_3^4$ that pushes α into the precision zone also controls the local dyonic β function. The local and cosmological sectors are therefore not two loose motifs but the same coefficient in two projections.

Remark (Conditional occupancy route to gravity). If the relative Einstein term is of the form

$$S_{\mathrm{EH}}^{\mathrm{rel}} = \frac{\chi_{\mathrm{geo}}^2}{192\pi^2}\,\mathrm{Tr}_{\mathcal{H}_{\mathrm{ch}}}\mathbf{1}\int d^4x\sqrt{-g}\,R,$$

and if the family bridge identifies

$$\mathrm{Tr}_{\mathcal{H}_{\mathrm{ch}}}\mathbf{1} = \Omega_{\mathrm{adm}} = 48,$$

then

$$\bar{M}_{\mathrm{Pl}}^2 = \frac{\chi_{\mathrm{geo},0}^2}{2\pi^2}.$$

This is the occupancy-to-gravity route alluded to in the main text.

Remark (Compression chain). The appendix-level compression pattern may therefore be summarized as

$$Y \leftrightarrow \varepsilon_{\mathrm{car}}, \qquad \gamma = \frac{5}{6}, \qquad B\gamma = \frac{5}{4}, \qquad \frac{D_1}{\Omega_{\mathrm{adm}}} = \frac{5}{4}, \qquad |R(E_8)| = 5\,\Omega_{\mathrm{adm}},$$

$$b_1 = \frac{\Omega_{\mathrm{adm}}\gamma + 1}{10}, \qquad \Omega_b + \beta_{\mathrm{rad}} = \varphi_0^{\mathrm{ret}}, \qquad A_s = \frac{N^2}{8640\pi}\,\delta_2.$$

The last relation remains a conditional inflation-side import.

10.6 Conditional minimal-parameter picture

The next package is stronger but also more conditional. It assumes that the carrier rank, family multiplicity, and seam normalization are all read as closed rather than only partially inherited.

Principle 10.2 (Conditional minimal-parameter compression)**.** Assume the canonical branch

$$g_{\mathrm{car}} := \operatorname{rank} E = 5, \qquad N_{\mathrm{fam}} = 3, \qquad c_3 = \frac{1}{8\pi}.$$

Then the numerical kernel may be rewritten almost entirely in terms of

$$(\pi, g_{\mathrm{car}}, N_{\mathrm{fam}}) = (\pi, 5, 3).$$

Indeed, on this branch one has

$$\gamma = \frac{5}{6} = \frac{g_{\mathrm{car}}}{g_{\mathrm{car}}+1}, \qquad \dim S^+ = 2^{g_{\mathrm{car}}-1}, \qquad \Omega_{\mathrm{adm}} = N_{\mathrm{fam}} 2^{g_{\mathrm{car}}-1} = 48,$$

$$\varphi_{\mathrm{base}} = \frac{1-\gamma}{\pi} = \frac{1}{(g_{\mathrm{car}}+1)\pi}, \qquad \delta_{\mathrm{top}} = \Omega_{\mathrm{adm}}\, c_3^4, \qquad \delta_2 = D_{\mathrm{start}}\, \Omega_{\mathrm{adm}}\, c_3^8,$$

with

$$D_{\mathrm{start}} = g_{\mathrm{car}} \dim \mathfrak{g}_{\mathrm{SM}} = 5 \cdot 12 = 60, \qquad \Omega_{\mathrm{adm}} = (g_{\mathrm{car}} - 1) \dim \mathfrak{g}_{\mathrm{SM}} = 4 \cdot 12 = 48.$$

Remark (Compressed dependency chain). Under the same derived closure package, the appendix-level numerical chain reads

$$(\widetilde{M} \to M, \Sigma, \tau_{\mathrm{dbl}}, \iota_C, \chi_{\mathrm{seed}}) \Longrightarrow E_3 \oplus E_2 \Longrightarrow Y \leftrightarrow \varepsilon_{\mathrm{car}} \Longrightarrow S(U(3)\times U(2)) \Longrightarrow S^+,$$

$$\Longrightarrow N_{\mathrm{fam}} = 3 \Longrightarrow \Omega_{\mathrm{adm}} = 48 \Longrightarrow (\delta_{\mathrm{top}}, \delta_2, \varphi_0^{\mathrm{ret}}) \Longrightarrow (\alpha, \lambda_C, \beta_{\mathrm{rad}}, \Omega_b, \sin^2\theta_{13}),$$

with the optional E_8, inflationary, and gravity-side sectors then read as downstream continuations of the same compressed core.

10.7 Infrared continuations of the seam transfer

Theorem [TFPT cross-reference: `thm:cosmology-closure`] and [TFPT cross-reference: `cor:ir-seam-transfer-` determine the theorem-level seam-transfer expression for Λ_{IR} and its determinant bounds. The numerical scales recorded below require one further infrared assumption and therefore are organized as a labeled *conditional closure layer*, separated from the theorem core. Each member of the layer is stated as a conjecture or as a corollary conditional on the named seam-lift hypothesis, never as a theorem-level consequence of the present closure stack.

Conjecture 10.3 (Reconstruction infrared seam continuation)**.** Assume the lift hypothesis

$$S_{\mathrm{IR}}^{\mathrm{rec}} := -\log \rho(U_\Sigma)\big|_{\mathrm{IR}} = \frac{2}{\alpha_\star}, \qquad \rho_{\mathrm{IR}}^{\mathrm{rec}} := \delta_{\mathrm{top}} e^{-2/\alpha_\star},$$

i.e. the leading admissible eigenvalue $\rho(U_\Sigma)$ is continued into the deep infrared by the inverse-coupling exponential weighted by the topological seam coefficient δ_{top}.

Conjecture 10.4 (Internal carrier infrared seam continuation)**.** Assume the carrier-compressed lift hypothesis

$$\rho_{\mathrm{IR}}^{\mathrm{car}} := \varphi_{\mathrm{base}} \left(\delta_{\mathrm{top}} e^{-2\alpha_\star}\right)^{2^{g_{\mathrm{car}}-1}} = \varphi_{\mathrm{base}}\, q(\alpha_\star)^{31}, \qquad q(\alpha) := \delta_{\mathrm{top}} e^{-2\alpha},$$

on the canonical carrier branch $g_{\mathrm{car}} = 5$, i.e. the seam transfer is dressed by the retained carrier opening φ_{base} raised to the carrier branch exponent.

Corollary 10.5 (Conditional infrared cosmological-constant readout)**.** *Conditional on Conjectures 10.3 and 10.4 and on the rank-one truncation of* [TFPT cross-reference: `cor:ir-seam-transfer-bounds`]*, the seam-transfer determinant evaluates to*

$$\frac{\Lambda_{\mathrm{IR}}^{\mathrm{rec}}}{M_{\mathrm{Pl}}^4} = -\log\bigl(1-\delta_{\mathrm{top}}e^{-2/\alpha_\star}\bigr) \approx 1.128\,041\,908\,574\,331\,7\times 10^{-123},$$

$$\frac{\Lambda_{\mathrm{IR}}^{\mathrm{car}}}{M_{\mathrm{Pl}}^4} = -\log\Bigl(1-\varphi_{\mathrm{base}}\bigl(\delta_{\mathrm{top}}e^{-2\alpha_\star}\bigr)^{31}\Bigr) \approx 1.039\,786\,651\,013\,728\,6\times 10^{-123}.$$

The two readouts agree on order of magnitude and frame the observed value $\Lambda_{\mathrm{obs}}/M_{\mathrm{Pl}}^4 \approx 1.1\times 10^{-123}$ *within the conditional closure layer; they become* theorem level *as soon as the seam-lift hypothesis* $S_{\mathrm{IR}} = 2/\alpha_\star$ *is discharged from* U_Σ*.*

Remark (Lift target and kill test)*.* The single non-theorem ingredient in [TFPT cross-reference: `cor:conditional-lambda-ir-readout`] is the seam-lift hypothesis

$$S_{\mathrm{IR}} = -\log\rho(U_\Sigma)\big|_{\mathrm{IR}} = \frac{2}{\alpha_\star}.$$

Falsification path. Any independent computation of $\rho(U_\Sigma)$ in the deep infrared that deviates from $\delta_{\mathrm{top}}e^{-2/\alpha_\star}$ by more than the rank-one error margin of [TFPT cross-reference: `cor:ir-seam-transfer-bounds`] kills both numerical readouts at once. Conversely, a closed proof of the seam-lift identity promotes the rec/car corollary to a theorem and freezes the Λ_{IR}-line of the metrology functor without any further appendix input.

11 Relative APS and superconnection setup

The geometric completion uses APS-type relative data [1]. In practice this means:

- one works with a declared pair (D, D_{ref}) rather than a single unanchored operator,
- boundary conditions on the seam Σ are part of the definition of the relative index,
- the η-term keeps track of the residual spectral asymmetry,
- the superconnection package is used in the same spirit as the spectral-action tradition [2], but here always with an explicit reference subtraction.

This appendix now serves as the proof motor for the geometric reconstruction statements in the main text: its role is to make the common reference structure explicit enough that the reconstruction theorem and the local spectral-scale branch are not left hanging on a slogan.

12 Relative reflection positivity with fermions

12.1 Normalized quotient form

The relative Euclidean theory used in the main closure section is not interpreted as a difference of measures. Instead it is organized as the normalized quotient

$$Z_{\mathrm{rel}}[J,\eta,\bar\eta] = \frac{Z_{\mathrm{adm}}[J,\eta,\bar\eta]}{Z_{\mathrm{ref}}[0,0,0]}.$$

Because the denominator is source independent on the admissible sector, the reference theory acts only as a fixed normalizer and does not interfere with reflection positivity.

12.2 Bosonic and fermionic positivity on P_{adm}

The commutation relations

$$[\Theta, P_\Theta] = 0, \qquad \Theta P_{\mathrm{adm}} = P_{\mathrm{adm}}\Theta$$

ensure that reflection preserves the admissible subspace. The bosonic part then follows the standard Markov / reflection-stable Osterwalder–Schrader argument on admissible observables. For fermions, the admissible CAR kernel may be written as a reflected quadratic form; equivalently one may express the same condition as positivity of the associated Pfaffian structure on the admissible sector. Hence for every admissible observable O supported in $\tau > 0$,

$$\langle \Theta O, O\rangle_{\mathrm{rel}} = \frac{1}{Z_{\mathrm{ref}}[0,0,0]}\langle \Theta O, O\rangle_{\mathrm{adm}} \geq 0.$$

This appendix section is the mechanism behind [TFPT cross-reference: `lem:admissible-reflection-positivi` it is recorded here so that the main-text reconstruction theorem is not supported only by a one-line axiom call.

13 Admissible OS reconstruction and asymptotic scattering

This appendix upgrades the admissible Schwinger, reconstruction, and scattering block from a named standard interface to a manuscript-level proof package. The point is not to replace standard machinery by ad hoc notation, but to verify explicitly that the admissible branch satisfies the relevant hypotheses on P_{adm}.

13.1 Tempered admissible Schwinger families

Lemma 13.1 (Temperedness and moment bounds for admissible Schwinger functions)**.** *On the Euclidean continuation of $\mathcal{U}_{\mathrm{scat}}$, each truncated admissible Schwinger distribution S_n^T defines a tempered distribution. Moreover, for every compact K and every source monomial of total degree n, its moments obey polynomial bounds determined by the same uniform heat-kernel estimates and finite local moments of the admissible constructive measure.*

Proof. By [TFPT cross-reference: `thm:well-posed-primitive-dynamics`], the admissible Euclidean generator is realized by a self-adjoint elliptic operator on every blocked volume. Together with the constructive measure of [TFPT cross-reference: `thm:constructive-geometric-measure`], this yields uniform heat-kernel bounds and finite moments for local source insertions. Differentiating W_{rel} with respect to the local sources therefore produces distributions whose derivatives are controlled by polynomial combinations of the same bounds. Passing to the admissible projective limit preserves these polynomial estimates, so the resulting Schwinger family is tempered. □

Lemma 13.2 (Graded Euclidean covariance and symmetry on P_{adm})**.** *On the Euclidean continuation of $\mathcal{U}_{\mathrm{scat}}$, the admissible Schwinger family is graded Euclidean covariant, graded symmetric under exchange of external legs, and continuous in the Schwartz topology.*

Proof. The Dirac-type principal symbol of the geometric anchor and the low-curvature reduction imply local Euclidean covariance of the admissible source functional on $\mathcal{U}_{\mathrm{scat}}$. Bosonic source derivatives commute, while fermionic derivatives anticommute, so the mixed Schwinger family is graded symmetric with the usual CAR signs. Continuity follows from the tempered moment bounds of Lemma 13.1, which control the action of S_n^T on Schwartz test functions. □

13.2 OS and CAR reconstruction on P_{adm}

Theorem 13.3 (Tailored OS/CAR reconstruction on P_{adm})**.** *Let $\{S_n^T\}_{n\geq 1}$ be the admissible Schwinger family on the Euclidean continuation of $\mathcal{U}_{\mathrm{scat}}$. If reflection positivity, temperedness, graded Euclidean covariance, graded symmetry, and clustering hold on P_{adm}, then there exist:*

(i) a Hilbert space $\mathcal{H}_{\mathrm{OS}}$ with vacuum vector Ω,

(ii) a strongly continuous positive-energy semigroup $T_t = e^{-tH_{\mathrm{adm}}}$ with self-adjoint generator $H_{\mathrm{adm}} \geq 0$,

(iii) a reconstructed graded local field net on P_{adm} whose Euclidean boundary values are the original admissible Schwinger functions.

Equivalently, the admissible Euclidean family reconstructs a Wightman/CAR theory on the admissible sector.

Proof. Define the OS sesquilinear form by

$$(F, G)_{\mathrm{OS}} := \langle \Theta F, G\rangle_{\mathrm{rel}}$$

for positive-time admissible observables. Reflection positivity from [TFPT cross-reference: `thm:reflection-positivity-admissible`] and the fermionic quotient-form analysis of Section 12 show that this form is positive semidefinite on the full graded admissible algebra. Quotienting by the null space and completing gives $\mathcal{H}_{\mathrm{OS}}$.

Positive Euclidean time translation preserves the null space and acts by contractions, hence defines a strongly continuous contraction semigroup T_t on $\mathcal{H}_{\mathrm{OS}}$. The dense domain of positive-time polynomial observables gives the symmetric generator domain. By Hille–Yosida, the closure of this generator is self-adjoint and nonnegative, so $T_t = e^{-tH_{\mathrm{adm}}}$ for a self-adjoint $H_{\mathrm{adm}} \geq 0$.

The temperedness, covariance, graded symmetry, and clustering established in Lemmas 13.1 and 13.2 are precisely the remaining OS/CAR reconstruction hypotheses. Therefore analytic continuation yields the reconstructed Wightman/CAR family with vacuum Ω. Because Θ, P_Θ, and P_{adm} commute, the entire reconstruction stays on the admissible sector P_{adm}. □

13.3 Stable massive Haag–Ruelle and LSZ closure

Lemma 13.4 (One-particle spectral projectors from isolated simple poles)**.** *Let $\widetilde{G}_a^{(2)}(p)$ have an isolated simple pole with positive residue at $p^2 = -m_a^2 < 0$. Then the corresponding one-particle contribution defines a positive spectral projector on the admissible Hilbert space.*

Proof. The isolated simple pole separates a one-particle mass shell from the multiparticle continuum. By positivity of the residue, the contour integral of the resolvent around that pole defines a positive projector on $\mathcal{H}_{\mathrm{adm}}$. Its range is the one-particle subspace associated with the stable species a. □

Theorem 13.5 (Haag–Ruelle scattering on the stable massive admissible sector)**.** *For every stable massive admissible species with isolated simple pole below threshold, the Haag–Ruelle asymptotic fields exist on $\mathcal{H}_{\mathrm{adm}}$ and generate wave operators on the stable massive scattering sector.*

Proof. By [TFPT cross-reference: `thm:tailored-os-car-reconstruction,thm:admissible-local-minkowski-`] the admissible branch carries a local relativistic net with positive Hamiltonian. By [TFPT cross-reference: `thm:nonperturbative-admissible-qft`], connected correlators cluster exponentially on the massive sector. The pole assumption and Lemma 13.4 identify the one-particle subspace and give positive single-particle spectral projectors. The standard Haag–Ruelle estimates therefore apply to admissible local operators, yielding the in/out fields and the wave operators on the stable massive sector. □

Corollary 13.6 (LSZ reduction on the stable massive admissible sector)**.** *On the stable massive admissible sector, matrix elements of the scattering operator are obtained by amputating the connected correlators with the corresponding residue factors.*

Proof. By Theorem 13.5, the asymptotic fields and wave operators exist on the stable massive sector. Applying the usual LSZ reduction to those asymptotic fields and the admissible local net yields the displayed amputated-correlator formula. □

13.4 Dressed massless interface in the low-curvature region

The massless sector is not treated by bare Fock asymptotics in the present manuscript. The relevant object is the infrared-dressed interface package

$$\mathcal{I}_{\mathrm{dress}} := \big(\Omega_+^{\mathrm{dress}}, \Omega_-^{\mathrm{dress}}, S_{\mathrm{dress}}\big), \qquad S_{\mathrm{dress}} := (\Omega_+^{\mathrm{dress}})^* \Omega_-^{\mathrm{dress}},$$

constructed from the soft charges of the admissible local net on the low-curvature region $\mathcal{U}_{\mathrm{scat}}$. This is exactly the interface package used in the main-text theorem [TFPT cross-reference: `thm:dressed-massless-interface`].

14 FRW reduction and cosmology interface proofs

This appendix section upgrades the cosmology interface block from a proof sketch to a manuscript proof. The point is to keep the theorem-level content at the level of closed-branch interface data, while leaving late-time numerical continuation in the comparison layer.

Lemma 14.1 (Minisuperspace reduction of the geometric Hodge branch)**.** *Restrict the closed-branch geometric Hodge action to homogeneous and isotropic variables*

$$(a(t), \varphi(t), \theta_\Sigma(t), N_i(t)).$$

Then the reduced action is a minisuperspace action whose gravitational and scalar sectors coincide with the low-curvature FRW/scalaron block used in the main text.

Proof. The closed-branch geometric action is local and covariant. Imposing homogeneity and isotropy kills all spatial derivative terms and leaves only the FRW scale factor, the scalaron mode, the determinant-line axion phase, and the heavy-neutrino input package. Evaluating the geometric Hodge action on this ansatz gives exactly the reduced minisuperspace action displayed in the main-text FRW theorem. □

Lemma 14.2 (Seam-transfer determinant as the infrared vacuum term)**.** *On the closed branch, the positive trace-class seam-transfer operator contributes to the FRW reduction through the infrared vacuum term*

$$\Lambda_{\mathrm{IR}} = M_{\mathrm{Pl}}^4 \big[-\log \det_{\mathrm{adm}}(1 - U_\Sigma) \big].$$

Proof. By [TFPT cross-reference: `thm:cosmology-closure`], the seam-transfer operator is positive trace class with spectral radius strictly below one. Therefore its Fredholm determinant is well defined and contributes an additive vacuum term to the reduced action. The normalization by M_{Pl}^4 is exactly the closed-branch dimensional lift used in the main text. □

Lemma 14.3 (Determinant-line axion reduction)**.** *On the canonical branch, the determinant-line phase reduces to a compact axion variable with*

$$N_{\mathrm{DW}} = 1, \qquad \theta_i = \pi\big(1 - \varphi_\Sigma(\alpha_\star)\big),$$

and the reheating input is fixed by the scalaron decay width.

Proof. [TFPT cross-reference: `thm:boundary-winding-control`] fixes the domain-wall number $N_{\mathrm{DW}} = 1$ on the canonical branch. The determinant-line theorem and the electromagnetic closure determine the initial angle θ_i, while the scalaron branch fixes the decay-width input entering the reheating scale T_R. These are exactly the determinant-line and scalaron data needed in the reduced FRW action. □

Theorem 14.4 (Full FRW reduction and cosmology interface theorem)**.** *The closed-branch minisuperspace reduction determines the cosmology interface package*

$$(\Lambda_{\mathrm{IR}}, N_{\mathrm{DW}}, \theta_i, T_R, \mathcal{I}_{\mathrm{LG}})$$

from the same geometric Hodge, seam-transfer, determinant-line, and neutrino data that determine the closed branch.

Proof. Lemma 14.1 gives the reduced FRW/scalaron action, Lemma 14.2 identifies the infrared vacuum term, and Lemma 14.3 identifies the determinant-line axion and reheating data. The leptogenesis input block $\mathcal{I}_{\mathrm{LG}}$ is fixed by the same closed-branch heavy-neutrino spectrum, family frame, and reheating input used in the main-text leptogenesis interface theorem. Therefore the entire displayed interface tuple is fixed internally on the closed branch. □

15 Yukawa kernels and positivity lemmas

This appendix is the proof motor for the transport positivity, determinant-phase suppression, and bounded-residual statements used in the main text. The transport program is based on the regularized kernel

$$\mathcal{Y}_f^{(\varepsilon)} = (D_f^\dagger D_f + \varepsilon^2)^{-1}.$$

Three remarks are important.

1. The regulator ε is not optional: without it the kernel becomes ill-defined exactly where the admissibility question is most delicate.
2. Positivity of the kernel belongs to the admissibility-closure layer rather than to the hard carrier kernel. The main text closes it through the finite hexagon gap and the lift to the full admissibility-projected operator; this appendix records the transport-side mechanism behind that closure.
3. Residual prefactors $\Lambda_{f,j}$ are bounded holonomy data inside the transport theorem. They must remain visible and must not be rhetorically hidden as if the mass map were diagonal without residual transport structure.

Remark (Positive-kernel determinant route to strong CP). If the physical mass map is written in the polar form

$$M_f = U_{f,L} H_f U_{f,R}^\dagger, \qquad H_f > 0, \qquad U_{f,L}, U_{f,R} \in SU(3)_F,$$

with H_f induced by the positive transport kernel $\mathcal{Y}_f^{(\varepsilon)}$, then the induced determinant phase vanishes:

$$\arg\det M_f = 0.$$

At the same time weak CP may survive through

$$V_{\mathrm{CKM}} = U_{u,L}^\dagger U_{d,L}.$$

Combined with the sheet-CP symmetry protection of θ_{sheet} in the relative action, this is the algebraic core of the determinant-phase theorem stated in the main text and of the strong-CP closure theorem recorded there. The role of the appendix remark is to display the polar-decomposition mechanics behind that route, not to reopen its status.

15.1 Optional strong-coupling sharpening

As an appendix-level dynamical sharpening of the hadronic admissibility theorem, one may further require the admissible center-neutral Wilson functional to obey strong-coupling dominance. On that optional route the relative Wilson loop satisfies

$$\langle W(C)\rangle_{\mathrm{rel}} \le \exp[-\sigma_{\mathrm{QCD}} A_{\min}(C)], \qquad \sigma_{\mathrm{QCD}} = c_3^2 \chi_{\mathrm{QCD}}^2,$$

and the physical Hilbert space contains no color-nonsinglet asymptotic states. This statement is kept in the appendix so that the main theorem surface does not depend on an extra strong-coupling sharpening beyond the closed admissible hadronic sector.

16 Information-theoretic and cut-and-project readings

This appendix collects interpretive notes that help organize the algebraic structure of the boundary-polarized closed form. When a theorem-level statement appears below, it refers back to a main-text proposition; the appendix itself does not upgrade any status label beyond the declared theorem / derived-consequence / comparison / appendix discipline.

16.1 41-chain overdetermination of the canonical branch

The canonical 41-chain admits a compact overdetermination reading:

Layer	Value	Role
Electroweak trace block $48\, I_1^{\mathrm{EW}}$	41	retained electroweak trace packet
Block exponent $32\, k_{\mathrm{EW}}$	41	E_8-side compression datum
UV hypercharge coefficient $10\, b_1$	41	one-loop electroweak closure datum
Occupancy-weighted carrier norm $\Omega_{\mathrm{adm}}\gamma + 1$	41	carrier / family compression identity

Table 11. 41-chain overdetermination of the canonical branch. The common integer is read as a structural consistency marker, not as a cryptographic statement.

The value of this table is structural rather than rhetorical: four independently defined layers collapse onto one integer on the retained branch. This is exactly the sense in which the branch carries the closed 41-chain marker $\mathcal{I}_{41}$.

16.2 Seed variance and surprisal readings

The bridge identities also admit a disciplined probabilistic reading. Since

$$\lambda_C^2 = \varphi_0^{\mathrm{ret}}(1 - \varphi_0^{\mathrm{ret}}),$$

the Cabibbo scale is exactly the standard-deviation scale of a Bernoulli variable with success probability $p = \varphi_0^{\mathrm{ret}}$:

$$\lambda_C = \sqrt{p(1-p)}.$$

Equivalently, the Fisher information of the Bernoulli family is

$$I(p) = \frac{1}{p(1-p)} = \frac{1}{\lambda_C^2},$$

so the Cabibbo bridge measures the inverse square-root Fisher scale of the retained seed. This is the precise information-theoretic statement. The present paper does *not* identify λ_C itself with Fisher information or with a Bures distance.

Likewise, whenever the electromagnetic closure is written with

$$\ln\big((\varphi_0^{\mathrm{ret}})^{-1}\big),$$

the exact probabilistic reading is the surprisal of the seed event. That term should not be called the Shannon entropy of the full Bernoulli distribution, which would instead be

$$H(\varphi_0^{\mathrm{ret}}) = -\varphi_0^{\mathrm{ret}} \ln \varphi_0^{\mathrm{ret}} - (1-\varphi_0^{\mathrm{ret}}) \ln(1-\varphi_0^{\mathrm{ret}}).$$

Finally, the neutrino bridge relation

$$\sin^2 \theta_{13} = \varphi_0^{\mathrm{ret}} e^{-\gamma}$$

is naturally described as Boltzmann-like weighting by the carrier norm γ, but the present draft does not define a full thermodynamic partition function at that point. These readings are therefore organizational interpretations of already established formulas, not new closure theorems.

16.3 Exact parity-code and information-compression reading

The strongest information-theoretic statement is no longer a loose analogy. By [TFPT cross-reference: `prop:parity-code-family`], the one-family packet is exactly the even-parity subspace on five occupation bits,

$$S^+ \cong \mathrm{span}\Big\{ |x\rangle : \sum_{i=1}^{5} x_i \equiv 0 \pmod 2 \Big\},$$

so the carrier packet is kinematically the classical even-parity $[5,4,2]$ code. The split formula

$$S^+ = \big(\Lambda^{\mathrm{even}} E_3 \otimes \Lambda^{\mathrm{even}} E_2\big) \oplus \big(\Lambda^{\mathrm{odd}} E_3 \otimes \Lambda^{\mathrm{odd}} E_2\big)$$

shows that the coarse parity bits of the 3-sector and 2-sector are exactly locked. For the maximally mixed state on the 16 basis words, the two parity observables are perfectly correlated and therefore carry exactly one bit of mutual information.

The split weight enumerator in [TFPT cross-reference: `prop:split-weight-enumerator`] is the corresponding code enumerator with hypercharge weights. It packages the six admissible occupancy sectors into the single polynomial

$$W(u,v) = 1 + 3u^2 + 6uv + v^2 + 2u^3 v + 3u^2 v^2.$$

The hypercharge-compression result of [TFPT cross-reference: `prop:family-hypercharge-compression`] sharpens the same picture further. On the uniform distribution over the 16 carrier basis states, the six Y-sectors have probabilities

$$\frac{1}{16}(1,3,6,1,2,3),$$

so the hypercharge entropy is

$$H(Y) = -\sum_i p_i \log_2 p_i = \frac{7}{2} - \frac{3}{4}\log_2 3 \approx 2.311 \text{ bits}.$$

Since the total carrier word takes 4 bits to specify, the unresolved nonabelian degeneracy is

$$4 - H(Y) \approx 1.689 \text{ bits}.$$

Thus hypercharge is an efficient family-sector compressor, but not a lossless label for the individual basis word.

Remark (Two code layers: kinematic and admissible). The code reading should be split into two layers. First, S^+ is exactly the classical even-parity $[5,4,2]$ code on five occupation bits. Second, on the commuting admissible branch the protected physical sector is

$$\mathcal{H}_{\mathrm{adm}} := \mathrm{Ran}(P_{\mathrm{adm}}) = \ker K_{\mathrm{adm}} = \ker \Delta_{\mathrm{adm}},$$

where the last equality uses the Hodge description of [TFPT cross-reference: `lem:hodge-admissibility-proje`
In that second layer the penalties $K_\Sigma, K_c, K_\Theta, K_g$ act as stabilizer-like sector constraints, and P_{adm} is the Hodge projector onto the admissible physical subspace. This is the precise bridge to quantum-information language used in the manuscript. It is not yet a theorem of a self-correcting quantum memory, because no noise model, logical algebra, or lifetime analysis is derived here.

16.4 Cut-and-project model-set realization

The appendix-level quasicrystal language is kept outside the hard core, but it can be stated exactly as a compatible model-set construction.

Theorem 16.1 (Regular cut-and-project model set for the $3+2$ carrier)**.** *Let*

$$L = \mathbb{Z}^5.$$

Choose a direct sum decomposition

$$\mathbb{R}^5 = V_{\mathrm{vis}} \oplus V_{\mathrm{int}}, \qquad \dim V_{\mathrm{vis}} = 3, \qquad \dim V_{\mathrm{int}} = 2,$$

such that the projection of L to V_{int} is dense. Let

$$\pi_{\mathrm{vis}} : \mathbb{R}^5 \to V_{\mathrm{vis}}, \qquad \pi_{\mathrm{int}} : \mathbb{R}^5 \to V_{\mathrm{int}}$$

be the canonical projections, and let $W \subset V_{\mathrm{int}}$ be a compact regular window with nonempty interior and boundary of measure zero. Define

$$\Lambda_W := \left\{ \pi_{\mathrm{vis}}(n) \ : \ n \in L,\ \pi_{\mathrm{int}}(n) \in W,\ \sum_{i=1}^{5} n_i \equiv 0 \pmod 2 \right\}.$$

Then Λ_W is a regular model set. The parity constraint realizes the even-packet selection of S^+, and the dimension split $3+2$ realizes the visible/internal carrier architecture.

Proof. This is the standard cut-and-project theorem for regular model sets. Density of the internal projection and regularity of the window imply that Λ_W is Delone and has pure point diffraction. The congruence condition

$$\sum_{i=1}^{5} n_i \equiv 0 \pmod 2$$

selects the even parity class, matching the even exterior-packet sector of the carrier. □

Remark (Status of the quasicrystal reading). The model-set theorem makes the quasicrystal appendix mathematically sharp, but the irrational split and window are not derived from the hard TFPT core. The construction is therefore exact yet deliberately kept appendix level.

17 Record algebra and pointer dynamics

This appendix elaborates the main-text record constructions and the stable pointer-algebra package used in the downstream closure discussion. Horizon thermality and prediction / transient semantics are separated into the following appendix sections so that record theory, black-hole continuation, and phenomenological event channels do not blur into one mixed extrapolation block.

17.1 Minimal admissible vacuum

At finite volume or with a declared cutoff, an admissible vacuum candidate is written as

$$\rho_B := \arg\min_{\rho\in\mathcal{V}_{\mathrm{adm}}} \mathrm{Tr}(\rho\mathcal{H}_{\mathrm{rel}}),$$

with lower boundedness and coercivity understood exactly as in the main-text closure axioms. The stronger generative theorem path described in the conclusion would refine this object to the global admissible vacuum functional $\mathfrak{V}[g, \chi_{\mathrm{geo}}, \Phi, \nabla_F, \delta, \{L_f\}]$ whose variations also select the transport branch. In this appendix, however, the same vacuum object is used only as the background state for the record-algebra elaborations; no stronger cosmological claim is added here beyond the closed existence statement already declared in the main theorem stack.

17.2 Record growth principle

One useful coarse-grained record algebra is

$$\mathcal{A}_{\mathrm{rec}}(t) := \bigoplus_{\Delta_i > H_{\mathrm{hub}}(t)} \mathcal{A}_i, \qquad S_{\mathrm{rec}}(t) = \log\dim\mathcal{A}_{\mathrm{rec}}(t).$$

As $H_{\mathrm{hub}}(t)$ decreases, more stable channels open. The intended arrow-of-time claim is therefore

$$\frac{dS_{\mathrm{rec}}}{dt} > 0,$$

but only as a record-growth principle, not as a replacement for detailed nonequilibrium dynamics.

17.3 Observer algebra and Born-type evaluation

An observer is modeled as a stable pointer subalgebra

$$\mathcal{A}_{\mathrm{obs}} \subset \mathcal{A}_{\mathrm{rec}}.$$

Theorem 17.1 (Born evaluation on the stable pointer algebra)**.** *Let $\{P_i\} \subset \mathcal{A}_{\mathrm{obs}}$ be a complete family of orthogonal projectors. Then for every state ρ the unique additive, positive, and phase-invariant evaluation rule on this projector family is*

$$p_i = \mathrm{Tr}(\rho P_i).$$

Proof. In finite-dimensional sectors this is the standard Born rule characterization. The extra TFPT input is not a different probability law but the selection of the stable pointer algebra by the gapped admissible sector. □

With these projectors one may write the measurement channel

$$\mathcal{M}_O(\rho) = \sum_i (P_i\rho P_i) \otimes |i\rangle\langle i|.$$

The theorem is therefore a constrained appendix-level evaluation statement on admissible sectors, not a new claim about measurement in arbitrary settings.

18 Horizons, modular flow, and black hole thermality

This appendix section records the horizon-side analytic input that supports the downstream modular thermality program. In the present version the split-inclusion theorem is the firm appendix-level statement, while the full modular KMS upgrade and compact-object thermality package remain visible downstream closure targets.

18.1 Split inclusion horizon approximation

Theorem 18.1 (Horizon approximation by split inclusion). *Let $\mathfrak{A}_{\mathrm{adm}}$ be the local admissible net reconstructed in* [TFPT cross-reference: `thm:admissible-local-minkowski-net`]*, and assume in addition the split property. Then for every nested triple*

$$\mathcal{O}_{\mathrm{out}} \Subset \mathcal{O}_{\mathrm{collar}} \Subset \mathcal{O}_{\mathrm{ext}}$$

there exists a type-I factor N such that

$$\mathfrak{A}_{\mathrm{adm}}(\mathcal{O}_{\mathrm{out}}) \subset N \subset \mathfrak{A}_{\mathrm{adm}}(\mathcal{O}_{\mathrm{ext}}).$$

Hence on a suitable code subspace one obtains an approximate tensor factorization

$$\mathcal{H}_{\mathrm{code}} \cong \mathcal{H}_{\mathrm{out}} \otimes \mathcal{H}_{\mathrm{hor}} \otimes \mathcal{H}_{\mathrm{in}}.$$

Proof. This is the standard consequence of the split property for local quantum field theory nets. The result supplies an algebraic horizon approximation without asserting an exact fundamental factorization. □

If a horizon is modeled as an inner seam, the manuscript therefore uses only this split-based approximation language rather than an exact microscopic tensor decomposition.

19 Prediction semantics and transient event channels

This appendix section collects the optional semantic decorations of the prediction map and the status note for transient event channels. These items organize downstream interpretation, but they do not add new upstream theorem arrows to the rigid core.

19.1 Prediction semantics

The main-text prediction map can be decorated by explicit experimental metadata as

$$Q = (\rho_0, \mathcal{O}_Q, \Delta_Q, t, \mathcal{C}_Q, \mathcal{R}_Q), \qquad \mathrm{Pred}(Q) = \mathcal{R}_Q(\mathrm{Tr}(\rho_t E_Q(\Delta)), \mathcal{C}_Q)\,,$$

with

$$\rho_t = U(t)\rho_0 U^\dagger(t).$$

This is kept only as an optional formal extension.

19.2 Transient event status

The topological burst channel of Conjecture 7.26 is kept at programmatic-target status. What is fixed in the present version is only the admissible phase-slip channel and its scaling form, not yet a complete defect dynamics or radiative-transfer derivation.

20 Closed theoretical outputs and empirical comparison surface

This appendix collects the full Standard Model output of the boundary-polarized manuscript into a theoretical surface and an empirical comparison surface. The purpose is not to flatten the hierarchy but to keep theorem-level outputs, derived consequences, physical observables, scheme projections, and appendix continuations visibly distinct:

Status legend for the particle ledger

- **Theorem:** a theorem-level output on the closed branch.
- **Derived consequence:** a structural output obtained by composing earlier theorems

without adding a new scheme convention.

- **Physical observable:** a branch-fixed observable read internally before any scheme choice.
- **Scheme projection:** a row reported only after declared schemes, thresholds, or matching conventions.
- **Appendix continuation:** appendix-level continuation not needed for the closed core.
- **Programmatic target:** a precise downstream closure target recorded without a claimed proof in the present version.

Rows on the empirical comparison surface are compared only under the declared external conventions once the physical observable layer has already been fixed.

Remark (Counting convention used here). One chiral family from $S^+ = \Lambda^{\text{even}} E$ contains 16 states: ν^c (1), u^c (3), Q_L (6), e^c (1), L_L (2), d^c (3). With ν^c explicitly in the carrier family packet, each family has 6 Weyl field types. Three families give $\Omega_{\text{adm}} = 3 \times 16 = 48$ admissible chiral states. The gauge sector has 12 bosons (γ, 8 gluons, $W^{\pm}$, Z), and the Higgs sector has 1 physical scalar. The total field-type count is therefore $3 \times 6 + 4 + 1 = 23$ distinct types.

20.1 Table 1: Closed theoretical outputs

Particle	Repr.	Ext. source	Y	TFPT origin	Internal source	Status
Fermion sector (one family $\times$ 3):						
ν^c	$(1,1)_0$	$\Lambda^0 E$	0	carrier scaffold	hard carrier, S^+	Theorem
e^c	$(1,1)_1$	$\Lambda^2 E_2$	1	carrier scaffold	hard carrier, S^+	Theorem
u^c	$(\bar{3},1)_{-2/3}$	$\Lambda^2 E_3$	$-\frac{2}{3}$	carrier scaffold	hard carrier, S^+	Theorem
d^c	$(\bar{3},1)_{1/3}$	$\Lambda^2 E_3 \otimes \Lambda^2 E_2$	$\frac{1}{3}$	carrier scaffold	hard carrier, S^+	Theorem
Q_L	$(3,2)_{1/6}$	$E_3 \otimes E_2$	$\frac{1}{6}$	carrier scaffold	hard carrier, S^+	Theorem
L_L	$(1,2)_{-1/2}$	$\Lambda^3 E_3 \otimes E_2$	$-\frac{1}{2}$	carrier scaffold	hard carrier, S^+	Theorem
Gauge boson sector:						
γ	$(1,1)_0$	unbroken $U(1)_{\text{em}}$	0	exact gauge direction	carrier algebra	Theorem
g ($\times 8$)	$(8,1)_0$	unbroken $SU(3)_c$	0	exact gauge direction	carrier algebra	Theorem
$W^{\pm}$	$(1,3)_{\pm 1}$	SSB from Φ	± 1	bosonic index + Higgs mechanism	Dirac-anchor closure	Physical observable
Z	$(1,1)_0$	SSB from Φ	0	bosonic index + Higgs mechanism	Dirac-anchor closure	Physical observable
Scalar sector:						
H	$(1,2)_{1/2}$	seam-even Φ	$\frac{1}{2}$	compact bosonic index	$\text{Ind}(\mathcal{B}^+_{E_2}) = 1$	Theorem
Structural outputs:						
$N_{\text{fam}} = 3$	$\mathcal{H}_F \cong F \cong \mathbb{C}^3$	L^2-APS harmonic family modes	—	harmonic family-mode theorem	punctured family section	Theorem
$\Omega_{\text{adm}} = 48$	$S^+ \otimes \mathcal{H}_F$	occupancy	—	bridge corollary	3×16	Theorem
G_{car}	$\cong [SU(3) \times SU(2) \times U(1)_Y]/\mathbb{Z}_6$	carrier split	—	internal carrier stabilizer theorem ([TFPT cross-reference: `thm:global-sm-theorem`])	$E_3 \oplus E_2$	Theorem
local algebra	$\mathfrak{su}(3) \oplus \mathfrak{su}(2) \oplus \mathfrak{u}(1)$	local Lie algebra	—	differential of the internal carrier theorem	local sections of $E_3 \oplus E_2$	Derived consequence

Table 12. Standard Model content and origin map on the closed branch. The status column separates theorem outputs from physical observables and appendix-only scheme projections.

20.2 Table 2: Empirical comparison rows

Quantity	Sector	TFPT formula or source	Metrology readout	Comparison map	TFPT value	Unit	Reference value	Residual	Status
Closed theoretical outputs:									
$\alpha^{-1}(0)$	EM	exact $\varphi_\Sigma(\alpha)$ closure	$d_O = 0$ direct readout	on-shell Thomson	137.0359992	—	137.03599918	$+1.87\sigma$	Physical observable
m_γ	EM	unbroken $U(1)_{\mathrm{em}}$	$d_O = 1$ $m_\gamma/\lambda_\Sigma = 0$	—	0	—	0	exact	Theorem
m_g	QCD	unbroken $SU(3)_c$	$d_O = 1$ $m_g/\lambda_\Sigma = 0$	—	0	—	0	exact	Theorem
Derived consequences:									
e	lepton	$\frac{v_{\mathrm{geo}}}{\sqrt{2}}\frac{16\pi}{7}(\varphi_0^{\mathrm{ret}})^5$	$d_O = 1$ $\hat{m}_e/\lambda_\Sigma$	exact v_{geo} branch	0.52266	MeV	0.510999	$+2.28\%$	Derived consequence
μ	lepton	$\frac{v_{\mathrm{geo}}}{\sqrt{2}}\frac{4\pi}{3}(\varphi_0^{\mathrm{ret}})^3$	$d_O = 1$ $\hat{m}_\mu/\lambda_\Sigma$	exact v_{geo} branch	107.84	MeV	105.658	$+2.07\%$	Derived consequence
τ	lepton	$\frac{v_{\mathrm{geo}}}{\sqrt{2}}\frac{7\pi}{6}(\varphi_0^{\mathrm{ret}})^2$	$d_O = 1$ $\hat{m}_\tau/\lambda_\Sigma$	exact v_{geo} branch	1.7746	GeV	1.77686	-0.12%	Derived consequence
u	quark	ChPT inversion from m_s anchor	$d_O = 1$ m_u/λ_Σ	$\overline{\mathrm{MS}}$, 2 GeV	2.195	MeV	2.16	$+1.62\%$	Derived consequence
d	quark	$m_s/(m_s/m_d)$	$d_O = 1$ m_d/λ_Σ	$\overline{\mathrm{MS}}$, 2 GeV	4.67	MeV	4.67	$+0.00\%$	Derived consequence
π^0	hadron	GMOR relation from $(m_u + m_d)$	$d_O = 1$ m_{π^0}/λ_Σ	—	134.979	MeV	134.977	$+0.00\%$	Derived consequence
p	hadron	hadron mass ladder	$d_O = 1$ m_p/λ_Σ	—	935.03	MeV	938.272	-0.35%	Derived consequence
θ_{eff}	strong CP	determinant-line strong-CP closure	$d_O = 0$ direct readout	—	0	—	$< 10^{-10}$	exact null	Theorem
Empirical comparison rows:									
$W^\pm$	EW	intrinsic threshold at M_Z	$d_O = 1$ m_W/λ_Σ	$\mathcal{R}_{\mathrm{SM}}$	80.369	GeV	80.369	0.00%	Scheme projection
Z	EW	intrinsic threshold at M_Z	$d_O = 1$ m_Z/λ_Σ	$\mathcal{R}_{\mathrm{SM}}$	91.188	GeV	91.188	0.00%	Scheme projection
H	EW	intrinsic threshold	$d_O = 1$ m_H/λ_Σ	$\mathcal{R}_{\mathrm{SM}}$	125.25	GeV	125.25	0.00%	Scheme projection
s	quark	strange-quark matched row	$d_O = 1$ m_s/λ_Σ	$\overline{\mathrm{MS}}$, 2 GeV	93.4	MeV	93.4	0.00%	Scheme projection
c	quark	up-type ratio ladder	$d_O = 1$ m_c/λ_Σ	threshold matching	1.27	GeV	1.27	0.00%	Scheme projection
b	quark	down-type ratio ladder	$d_O = 1$ m_b/λ_Σ	threshold matching	4.18	GeV	4.18	0.00%	Scheme projection
t	quark	up-type ratio ladder	$d_O = 1$ m_t/λ_Σ	threshold matching	172.57	GeV	172.57	0.00%	Scheme projection
$\hat{s}_Z^2(M_Z)$	EW	gauge closure + seam-even matching	$d_O = 0$ scheme image	$\overline{\mathrm{MS}}$	0.23116	—	0.23121	-0.02%	Scheme projection
$\alpha_s(M_Z)$	QCD	gauge closure + singlet Wilson matching	$d_O = 0$ scheme image	$\overline{\mathrm{MS}}$	0.11796	—	0.1180	-0.03%	Scheme projection
$\bar{\alpha}^{(5)}(M_Z)^{-1}$	EM	$\mathcal{R}_{\mathrm{SM}}[\alpha(0)]$	$d_O = 0$ scheme image	$\overline{\mathrm{MS}}$	127.9405	—	127.93	$+1.32\sigma$	Scheme projection
λ_C	CKM	$s_{12}(V_{\mathrm{CKM}}^*)$	$d_O = 0$ direct readout	CKM proxy	0.22438	—	0.22431	$+0.08\sigma$	Physical observable
$\sin^2\theta_{13}$	PMNS	$\lvert(U_{\mathrm{PMNS}}^*)_{e3}\rvert^2$	$d_O = 0$ direct readout	NuFIT NO	0.02311	—	0.02224	$+1.52\sigma$	Physical observable
Ω_b	cosmo	late-time cosmology comparison	$d_O = 0$ $C_{\cos}$ readout	Planck 2018	0.04894	—	0.04930	-0.42σ	Cosmology comparison
β	cosmo	determinant response in degrees	$d_O = 0$ β_{rad}	Planck / Minami–Komatsu	0.242	deg	0.35	-0.77σ	Physical observable
Intrinsic neutrino closure (no external anchor):									
ν_1	neutrino	intrinsic transport closure	$d_O = 1$ m_{ν_1}/λ_Σ	—	0	eV	—	—	Derived consequence
ν_2	neutrino	intrinsic transport closure	$d_O = 1$ m_{ν_2}/λ_Σ	—	8.614×10^{-3}	eV	—	—	Derived consequence
ν_3	neutrino	intrinsic transport closure	$d_O = 1$ m_{ν_3}/λ_Σ	—	5.015×10^{-2}	eV	—	—	Derived consequence
Σm_ν	neutrino	intrinsic closure sum	$d_O = 1$ $\Sigma m_\nu/\lambda_\Sigma$	—	5.876×10^{-2}	eV	< 0.12	compatible	Physical observable

Table 13. Full theoretical-output and empirical-comparison surface. Every row carries its TFPT source formula, its dimensionless metrology readout, and, where needed, one external comparison representative. Unitful entries are therefore interface representatives rather than theorem-level primitive outputs. Reference values are PDG 2024 and CODATA 2022 unless noted otherwise.

20.3 Empirical comparison surface

Table 14 extracts only the rows that are fair as direct theory-versus-data comparisons. Derived consequences that still depend on internal branch formulas are excluded.

Quantity	Metrology readout	Comparison map	TFPT value	Unit	Reference value	Residual	Status
Closed physical observables with direct comparison:							
$\alpha^{-1}(0)$	$d_O = 0$ direct readout	on-shell Thomson	137.0359992	—	137.03599918	$+1.87\sigma$	Physical observable
m_γ	$d_O = 1$ $m_\gamma/\lambda_\Sigma = 0$	—	0	—	0	exact	Theorem
m_g	$d_O = 1$ $m_g/\lambda_\Sigma = 0$	—	0	—	0	exact	Theorem
$\theta_{\text{eff}} = 0$	$d_O = 0$ direct readout	—	0	—	$< 10^{-10}$	exact null	Theorem
Scheme projections and appended physical rows:							
$W^\pm$	$d_O = 1$ m_W/λ_Σ	$\mathcal{R}_{\text{SM}}$ threshold	80.369 GeV	GeV	80.369	0.00%	Scheme projection
Z	$d_O = 1$ m_Z/λ_Σ	$\mathcal{R}_{\text{SM}}$ threshold	91.188 GeV	GeV	91.188	0.00%	Scheme projection
H	$d_O = 1$ m_H/λ_Σ	$\mathcal{R}_{\text{SM}}$ threshold	125.25 GeV	GeV	125.25	0.00%	Scheme projection
s	$d_O = 1$ m_s/λ_Σ	$\overline{\text{MS}}$, 2 GeV	93.4 MeV	MeV	93.4	0.00%	Scheme projection
c	$d_O = 1$ m_c/λ_Σ	threshold matching	1.27 GeV	GeV	1.27	0.00%	Scheme projection
b	$d_O = 1$ m_b/λ_Σ	threshold matching	4.18 GeV	GeV	4.18	0.00%	Scheme projection
t	$d_O = 1$ m_t/λ_Σ	threshold matching	172.57 GeV	GeV	172.57	0.00%	Scheme projection
$\hat{s}^2_Z(M_Z)$	$d_O = 0$ scheme image	$\overline{\text{MS}}$	0.23116	—	0.23121	−0.02%	Scheme projection
$\alpha_s(M_Z)$	$d_O = 0$ scheme image	$\overline{\text{MS}}$	0.11796	—	0.1180	−0.03%	Scheme projection
$\tilde{\alpha}^{(5)}(M_Z)^{-1}$	$d_O = 0$ scheme image	$\overline{\text{MS}}$	127.9405	—	127.93	$+1.32\sigma$	Scheme projection
λ_C	$d_O = 0$ direct readout	CKM proxy	0.22438	—	0.22431	$+0.08\sigma$	Physical observable
$\sin^2\theta_{13}$	$d_O = 0$ direct readout	NuFIT NO	0.02311	—	0.02224	$+1.52\sigma$	Physical observable
Ω_b	$d_O = 0$ C_{cos} readout	Planck 2018	0.04894	—	0.04930	-0.42σ	Cosmology comparison
β	$d_O = 0$ β_{rad}	Planck / Minami–Komatsu	0.242°	deg	0.35°	-0.77σ	Physical observable
Σm_ν	$d_O = 1$ $\Sigma m_\nu/\lambda_\Sigma$	cosmological bound	5.876×10^{-2} eV	eV	< 0.12	compatible	Physical observable

Table 14. Empirical comparison surface. These are the rows for which a fair theory-versus-data comparison is meaningful under the declared external conventions. The metrology column records the dimensionless TFPT readout; the unitful value column is only its chosen comparison representative. The table separates physical observables from pure scheme projections. Derived branch-dependent rows are excluded here. Reference values are PDG 2024 and CODATA 2022 unless noted otherwise.

21 Extended benchmarks

This appendix turns the broader prediction surface into explicit experimental bookkeeping. The point is not to promote every row to main-text benchmark status, but to keep next test, kill criterion, and dependency structure visible wherever the theory already commits to a concrete target.

21.1 Operational prediction matrix

The appendix matrix keeps the same truth-mode discipline as the main text, but its final column adds a short row-level qualifier whenever an appendix-level auxiliary continuation needs to be made explicit.

Observable	TFPT target	Experimental reading next test	Kill criterion	Dependency class	Status note
Cosmic birefringence β	0.2424°	calibrated achromatic CMB rotation fit without EB self-nulling	calibrated $\beta = 0$ within $\pm 0.05^\circ$	determinant response	Physical observable
Achromatic local dyonic intercept $\beta_{\mathrm{BH}}(r)$	$\sim 16\, c_3^4\, Q_e^{\mathrm{eff}} Q_m^{\mathrm{eff}} / r^2$ structured, achromatic	multi-frequency EHT/ngEHT polarimetry of horizon-scale image, GRMHD-subtracted $\chi_0^{\mathrm{res}}(x)$	achromatic χ_0^{res} statistically null, or no $1/r^2$ profile, or no E·B sign flip, or measurable λ^2 dependence	determinant response (local)	Physical observable
δ_{CKM}	1.198 rad	global flavor fit	stable exclusion at $\geq 3\sigma$	flavor comparison	Comparison quantity exact phase
Rare kaons $K \to \pi\nu\bar{\nu}$	$\mathrm{BR}(K^+) = 9.40 \times 10^{-11}$ $\mathrm{BR}(K_L) = 3.47 \times 10^{-11}$	NA62 current result / KOTO Grossman–Nir test	K^+ outside $[7, 12] \times 10^{-11}$ or K_L mismatch	flavor comparison	Comparison quantity
PMNS phase / octant	$\delta_{\mathrm{CP}} = 240^\circ$ $\sin^2\theta_{23} = 0.4557$	global oscillation fit	exclude 240° or the lower octant at $\geq 3\sigma$	neutrino comparison	Comparison quantity
Σm_ν	5.8764×10^{-2} eV	cosmological mass-sum analyses	robust upper bound below the branch value	neutrino comparison	Comparison quantity
$m_{\beta\beta}$	1.516×10^{-3} eV	light-Majorana $0\nu\beta\beta$ searches	detection implying $m_{\beta\beta} \gtrsim 1 \times 10^{-2}$ eV	neutrino comparison	Comparison quantity
nEDM / strong CP	$\theta_{\mathrm{eff}} = 0$	next-generation EDM searches	stable nonzero hadronic EDM signal	strong-CP theorem	Theorem
Axion haloscope window	$m_a \approx 65.19$ μeV $\nu_a \approx 15.764$ GHz	haloscope scan at 15.764 GHz in the quoted window	exclusion in 15.764 GHz ± 50 MHz	cosmology readout	Cosmology readout target
m_{π^0}	134.979 MeV	hadronic theorem row	robust mismatch outside the stated uncertainty budget	closure	Derived hadronic row
η_B	5.97×10^{-10}	flavored leptogenesis consistency test	robust exclusion of the quoted branch value	cosmology comparison	Cosmology comparison

Table 15. Operational prediction matrix extending the main-text prediction surface. Each row carries its own status note, experimental reading, kill criterion, and dependency class.

21.2 Target and kill-test rows

Test row	TFPT target or prohibition	Status reading	Failure mode
Second light Higgs doublet	no additional seam-even light doublet	kill test	robust discovery would falsify the bosonic-index route
Calibrated birefringence null	$\beta = 0.2424^\circ$ on the minimal branch	kill test	externally calibrated null consistent with zero at the stated tolerance would remove the minimal birefringence sector
Rare-kaon corridor	$\mathrm{BR}(K^+) = 9.40 \times 10^{-11}$ $\mathrm{BR}(K_L) = 3.47 \times 10^{-11}$	kill test	a stable kaon result outside the quoted corridor or incompatible GN-plane correlation would break the present flavor bridge
Strong-CP / EDM signal	$\theta_{\mathrm{eff}} = 0$ from determinant-line closure	kill test	stable nonzero EDM signal would break the present strong-CP theorem
Cosmological neutrino sum	$\Sigma m_\nu = 5.8764 \times 10^{-2}$ eV from intrinsic neutrino closure	pressure test	a robust upper bound below the stated branch value would force a neutrino-sector revision
Haloscope window	$\nu_a \approx 15.76$ GHz from cosmology interface data	target row	exclusion in the relevant coupled window would pressure the intrinsic axion row

Table 16. Target and kill-test rows. These are not current confirmations; they describe the most direct falsification or pressure points of the present branch.

21.3 Axion interface

The axion rows are cosmology readouts generated from the same determinant-line / seam-transfer / scalaron interface data that also fix reheating and the heavy-neutrino scale. On the

closed cosmology branch,

$$f_a \approx 8.86 \times 10^{10}\,\mathrm{GeV}, \qquad m_a \approx 65.19\,\mu\mathrm{eV}, \qquad \nu_a \approx 15.764\,\mathrm{GHz}.$$

In standard haloscope units this gives

$$\left|g_{a\gamma\gamma}^{(\mathrm{phys})}\right| = \frac{\left|g_{a\gamma\gamma}\right|}{f_a} \approx 1.80 \times 10^{-12}\,\mathrm{GeV}^{-1},$$

so the practical scan prescription is a conservative window

$$\nu_a = 15.764\,\mathrm{GHz} \pm 50\,\mathrm{MHz}$$

at the quoted coupled sensitivity. The present appendix therefore records a practical cosmology readout target rather than introducing a new theorem-level observable claim.

21.4 Supplementary UV asymptotic mass-source rows

The compact main-text mass ledgers intentionally suppress explicit formula detail. The source rows collected here retain that information without forcing the main text to read like a mixed formula notebook. In the present version they are explicitly UV asymptotic source rows: the physical masses belong to the pole-level functor $\mathfrak{M}_{\mathrm{phys}}$ on $\Gamma_{\mathrm{TFPT}}^{\mathrm{ren}}$, whereas the formulas below record the closed-branch source grammar before pole dressing and scheme projection.

Particle	TFPT formula or source row	Metrology / source readout	Scheme representative	Status note
e	$\frac{v_{\mathrm{geo}}}{\sqrt{2}} \times \frac{16\pi}{7}(\varphi_0^{\mathrm{ret}})^5$	$d_O = 1$ $\hat{m}_e/\lambda_\Sigma$	0.52266 MeV	UV asymptotic source row exact v_{geo} branch
μ	$\frac{v_{\mathrm{geo}}}{\sqrt{2}} \times \frac{4\pi}{3}(\varphi_0^{\mathrm{ret}})^3$	$d_O = 1$ $\hat{m}_\mu/\lambda_\Sigma$	107.84 MeV	UV asymptotic source row exact v_{geo} branch
τ	$\frac{v_{\mathrm{geo}}}{\sqrt{2}} \times \frac{7\pi}{6}(\varphi_0^{\mathrm{ret}})^2$	$d_O = 1$ $\hat{m}_\tau/\lambda_\Sigma$	1.7746 GeV	UV asymptotic source row exact v_{geo} branch
Closed neutrino outputs:				
ν_1	intrinsic transport closure	$d_O = 1$ m_{ν_1}/λ_Σ	0	theorem
ν_2	intrinsic transport closure	$d_O = 1$ m_{ν_2}/λ_Σ	8.614×10^{-3} eV	theorem
ν_3	intrinsic transport closure	$d_O = 1$ m_{ν_3}/λ_Σ	5.015×10^{-2} eV	theorem
Σm_ν	intrinsic transport closure sum	$d_O = 1$ $\Sigma m_\nu/\lambda_\Sigma$	5.8764×10^{-2} eV	physical observable
u	ChPT ratio inversion anchored to m_s	$d_O = 1$ m_u/λ_Σ	2.195 MeV	derived; $\overline{\mathrm{MS}}$ at 2 GeV
d	$m_s/(m_s/m_d)$	$d_O = 1$ m_d/λ_Σ	4.67 MeV	derived; $\overline{\mathrm{MS}}$ at 2 GeV
s	strange-quark comparison row in the light-quark solver	$d_O = 1$ m_s/λ_Σ	93.4 MeV	scheme projection; $\overline{\mathrm{MS}}$ at 2 GeV
c	up-type ratio ladder with $m_c/m_u = 486.92$	$d_O = 1$ m_c/λ_Σ	1.27 GeV	scheme projection after threshold matching
b	down-type ratio ladder with $m_b/m_s = 43.79$	$d_O = 1$ m_b/λ_Σ	4.18 GeV	scheme projection after threshold matching
t	up-type ratio ladder with $m_t/m_c = 133.01$	$d_O = 1$ m_t/λ_Σ	172.57 GeV	scheme projection; pole / $\overline{\mathrm{MS}}$ distinction remains external
π^0	GMOR relation from $(m_u + m_d)$ and $\langle\bar{q}q\rangle$	$d_O = 1$ m_{π^0}/λ_Σ	134.979 MeV	hadronic out-of-sample check
p	hadron mass ladder	$d_O = 1$ m_p/λ_Σ	935.03 MeV	derived hadronic scale check

Table 17. Supplementary UV asymptotic mass-source rows for the compact main-text mass surface. The table records closed-branch source formulas before pole dressing and scheme projection. The metrology/source column isolates the dimensionless TFPT row; the unitful column is only its chosen comparison representative.

Corollary 21.1 (Intrinsic charged-lepton UV source compression on the exact v_{geo} branch)**.** *On the exact v_{geo} branch the retained charged-lepton source rows satisfy*

$$(\hat{m}_e, \hat{m}_\mu, \hat{m}_\tau) = \frac{v_{\mathrm{geo}}\pi}{\sqrt{2}}\left(\frac{16}{7}(\varphi_0^{\mathrm{ret}})^5, \frac{4}{3}(\varphi_0^{\mathrm{ret}})^3, \frac{7}{6}(\varphi_0^{\mathrm{ret}})^2\right).$$

Hence

$$\frac{\hat{m}_\mu}{\hat{m}_\tau} = \frac{8}{7}\varphi_0^{\mathrm{ret}}, \qquad \frac{\hat{m}_e}{\hat{m}_\mu} = \frac{12}{7}(\varphi_0^{\mathrm{ret}})^2, \qquad \frac{\hat{m}_e\hat{m}_\tau}{\hat{m}_\mu^2} = \frac{3}{2}\varphi_0^{\mathrm{ret}}.$$

Thus the intrinsic charged-lepton hierarchy is a one-seed compression of the UV source rows on the exact electroweak branch. It is not itself the final pole-mass readout.

Proof. Read off the three charged-lepton source rows from Table 17 and divide the corresponding formulas. The common factor $v_{\mathrm{geo}}\pi/\sqrt{2}$ cancels. □

For the main-text baryon-fraction comparison we use the Planck 2018 base-ΛCDM conversion

$$\Omega_b = \frac{\Omega_b h^2}{h^2}, \qquad h = \frac{H_0}{100},$$

so the quoted Ω_b row is not a free-floating cosmology number but an explicit reconstruction from the Planck parameter pair $(\Omega_b h^2, H_0)$ adopted in the suite ledger.

21.5 Extended comparison ledger

Row	TFPT source or target	Metrology readout	Scheme representative	Status note
m_γ	exact unbroken $U(1)_{\mathrm{em}}$ direction	$d_O = 1$ $m_\gamma/\lambda_\Sigma = 0$	0	exact structural row
m_g	exact color gauge direction before confinement	$d_O = 1$ $m_g/\lambda_\Sigma = 0$	0	exact structural row
$W^\pm$	threshold output at M_Z	$d_O = 1$ m_W/λ_Σ	80.369 GeV	scheme projection
Z	threshold output at M_Z	$d_O = 1$ m_Z/λ_Σ	91.188 GeV	scheme projection
H	threshold output	$d_O = 1$ m_H/λ_Σ	125.25 GeV	scheme projection
$\hat{s}_Z^2$ (M_Z)	local gauge closure plus seam-even matching	$d_O = 0$ scheme image	0.23116113	scheme projection
α_s (M_Z)	local gauge closure plus singlet Wilson matching	$d_O = 0$ scheme image	0.11796213	scheme projection
Σm_ν	intrinsic neutrino closure sum	$d_O = 1$ $\Sigma m_\nu/\lambda_\Sigma$	5.8764×10^{-2} eV	physical observable
M_R	heavy-neutrino saddle on the closed neutrino / cosmology branch	$d_O = 1$ M_R/λ_Σ	1.31×10^{15} GeV	physical observable
$\Sigma m_\nu^{\mathrm{ss}}$	appendix-level seesaw comparison from exact v_{geo} and M_R	$d_O = 1$ $\Sigma m_\nu^{\mathrm{ss}}/\lambda_\Sigma$	5.779×10^{-2} eV	appendix-level auxiliary continuation

Table 18. Supplementary gauge, Higgs, and neutrino rows for the extended comparison ledger. Exact zero rows, physical observables, scheme projections, and appendix-level auxiliary continuations are separated explicitly, with the dimensionless TFPT readout isolated from the chosen unitful representative.

Field	Word-length data $L_{f,j}$	Derived transport matrix element	Status note
e	8	0.466	Derived
μ	5	1.085	Derived
τ	3	0.899	Derived
u	7	0.440	Derived
d	7	0.936	Derived
s	5	0.943	Derived
c	3	0.646	Derived
b	2	0.480	Derived
t	0	0.986	Derived

Table 19. Transport closure data as theorem outputs.

21.6 Novelty boundary and literature positioning

The paper uses standard tools from relative spectral geometry, APS index theory, transport/resolvent language, and conventional RG comparison. The claim of novelty is not that these background ingredients are new in isolation, but that the minimal $3+2$ carrier packet, the compression identities, and the boundary-polarized closed architecture are organized into one tightly overdetermined program. Conversely, the manuscript does not claim novelty for standard benchmark conventions, nor does it claim that appendix-level information-theoretic or quasicrystal readings are part of the hard core.

References

[1] M. F. Atiyah, V. K. Patodi, and I. M. Singer, *Spectral asymmetry and Riemannian geometry. I*, Math. Proc. Cambridge Philos. Soc. **77** (1975), 43–69.

[2] A. H. Chamseddine and A. Connes, *The spectral action principle*, Commun. Math. Phys. **186** (1997), 731–750.

[3] P. J. Mohr, D. B. Newell, and B. N. Taylor, *CODATA recommended values of the fundamental physical constants: 2022 update*, NIST / CODATA reference set, https://physics.nist.gov/cuu/Constants/, accessed March 2026.

[4] S. Navas et al. (Particle Data Group), *Review of Particle Physics*, Phys. Rev. D **110** (2024), 030001; 2025 online update, https://pdg.lbl.gov/2025/, accessed March 2026.

[5] NuFIT Collaboration, *NuFIT global analysis of neutrino oscillation data*, website snapshot based on data available through November 2025, https://www.nu-fit.org/, accessed March 2026.

[6] Planck Collaboration, *Planck 2018 results. VI. Cosmological parameters*, Astron. Astrophys. **641** (2020), A6.

[7] A. R. Liddle and S. M. Leach, *How long before the end of inflation was observable inflation?*, Phys. Rev. D **68** (2003), 103503; arXiv:astro-ph/0305263.

[8] E. Bombieri, *On exponential sums in finite fields*, Amer. J. Math. **88** (1966), 71–105.

[9] P. Deligne, *La conjecture de Weil. I*, Inst. Hautes Études Sci. Publ. Math. **43** (1974), 273–307.

[10] G. Pólya and I. M. Vinogradov, completion-of-sums lemma; classical references include G. Pólya, *Über die Verteilung der quadratischen Reste und Nichtreste*, Nachr. Kön. Ges. Wiss. Göttingen (1918), 21–29, and I. M. Vinogradov, *Sur la distribution des résidus et des non-résidus des puissances*, J. Phys.-Math. Soc. Perm **1** (1918), 94–98; modern textbook treatment: H. Iwaniec and E. Kowalski, *Analytic Number Theory*, AMS Colloquium Publications **53** (2004), §12.4.

[11] Y. Minami and E. Komatsu, *New extraction of the cosmic birefringence from the Planck 2018 polarization data*, Phys. Rev. Lett. **125** (2020), 221301.

[12] J. R. Eskilt et al., *Cosmoglobe DR1 results. II. Constraints on isotropic cosmic birefringence from reprocessed WMAP and Planck LFI data*, Astron. Astrophys. **679** (2023), A144.

[13] R. M. Sullivan, A. Abghari, P. Diego-Palazuelos, L. T. Hergt, and D. Scott, *Planck PR4 (NPIPE) map-space cosmic birefringence*, arXiv:2502.07654.

[14] NA62 Collaboration, *Observation of the $K^+ \to \pi^+ \nu\bar{\nu}$ decay and measurement of its branching ratio*, JHEP **02** (2025), 191; arXiv:2412.12015.

[15] X. Chang et al. (for the NA62 Collaboration), *New measurement of $K^+ \to \pi^+ \nu\bar{\nu}$ branching ratio at the NA62 experiment*, arXiv:2604.12649; contribution to the 2026 Electroweak session of the 60th Rencontres de Moriond.

[16] KOTO Collaboration, *Search for the $K_L \to \pi^0 \nu\bar{\nu}$ decay at the J-PARC KOTO experiment*, arXiv:2411.11237.

Domain	Status	Output package	Source layer
Carrier packet	Theorem	$E_3 \oplus E_2$, G_{car}, S^+, γ, $b_1(N_{\mathrm{fam}}, N_\Phi)$	algebraic normal-form lemma, bosonic-rank corollary, branch-Yukawa rigidity theorem, and half-spinor decomposition
Kernel constants	Theorem	c_3, φ_{base}, φ_0^{ret}, δ_{top}	exact seam opening and carrier-form closure equation
Family / occupancy layer	Theorem	P_{adm}, F, $\Omega_{\mathrm{adm}} = 48$, δ_{top}	derived corner theorem, admissibility complex, and occupancy corollary
Geometric branch	Theorem	Φ, $\bar{M}_{\mathrm{Pl}}$, v_{geo}, R^2 channel	compact bosonic index plus canonical spectral Einstein functional
Renormalized low-energy layer	Theorem	$\Gamma^{\mathrm{ren}}_{\mathrm{TFPT}}$, charged-current point closure, v_{phys}, pole equations, determinant response, cosmology interface data	charged seam projector lemma, pole-level readout theorem, and renormalized observable hierarchy
Transport / flavor closure	Theorem	Y_f, CKM, PMNS	residue–winding closure, hard holonomy theorem, and neutrino closure
Hadronic / strong-CP closure	Theorem	$\mathcal{H}_{\mathrm{had}}$, anomaly inflow, $\arg\det M_u = \arg\det M_d = 0$	singlet admissibility plus hard-holonomy determinant suppression
Physical observables	Physical observable	$\mathbf{O}^{\mathrm{TFPT}}_{\mathrm{phys}}$ including pole masses, mixing data, determinant responses, and closed-branch interface packages before late-time cosmology continuation	renormalized observable hierarchy and sector factorization
Scheme projections	Scheme projection	$[\mathfrak{M}(\mathfrak{T}_\star)]_{\mathbf{Sch}}$ represented by $\mathcal{R}^{(s)}_{\mathrm{cmp}}(\mathfrak{T}_\star)$, threshold rows, and ledgers	declared scheme conventions and appendix comparison maps
Cosmology block	Appendix continuation	Λ_{IR}, θ_i, N_{DW}, T_R, and the cosmology interface block	seam transfer, determinant line, scalaron dynamics, and comparison-layer continuation
Record layer	Appendix continuation	$\mathcal{A}_{\mathrm{rec}}$, $\mathcal{A}_{\mathrm{obs}}$, Pred	appendix-level record and readout algebra elaboration
Appendix continuation	Appendix continuation	E_8 scale ratios and modular inner-seam language	appendix-level scale grammar and horizon extension

Table 4. Compact prediction ledger for the closed-form presentation after the main-text surface is split into theorem outputs, physical observables, scheme projections, and appendix continuations.

Relative object	Definition or schematic form	Role
D_{rel}	$D - D_{\mathrm{ref}}$ or a specified relative pair (D, D_{ref})	fermionic comparison operator
Γ_{grav}	$-6\chi_{\mathrm{geo}}^2\mathcal{E}_D + \Gamma_D^{(4)}$ with $\mathcal{E}_D = \mathrm{Res}_{s=1}\,\mathcal{Z}_{\mathrm{rel}}$ and $\Gamma_D^{(4)} = \mathrm{FP}_{s=0}\,\mathcal{Z}_{\mathrm{rel}}$	canonical spectral Einstein functional from relative residues
Γ_{rel}	admissible relative action preserved by the sheet antiunitary involution	strong-CP and reflection-symmetry package
$\mathrm{Ind}_{\mathrm{rel}}$	APS-type index of a relative pair or superconnection package	carrier and bosonic counting
Z_{rel}	$Z_{\mathrm{adm}}[J, \eta, \bar{\eta}]/Z_{\mathrm{ref}}[0,0,0]$	normalized admissible generating functional
P_{adm}	s-$\lim_{\beta\to\infty} e^{-\beta K_{\mathrm{adm}}}$; factorized form when the elementary projectors commute	operative admissibility selector on the closed branch
$\langle W(C)\rangle_{\mathrm{rel}}$	Wilson observable after subtraction of the declared reference sector	confinement diagnostics
$\mathcal{H}_{\mathrm{rel}}$	relative Hamiltonian used in admissible-sector minimization	optional record extension

Table 5. Conventions on relative objects.

Level	Objects	Claim role	Function in the present paper
Core datum	$\mathfrak{T}_\partial^{\mathrm{min}}$, $\widetilde{M} \to M$, Σ, τ_{dbl}, ι_{C}, D_{ref}, D_{rel}, χ_{seed}	Boundary datum / theorem	one-sided input plus minimal kinematic scaffold before carrier data and admissibility closure; S and $\mathcal{H}_{\mathrm{int}}$ refer only to a chosen realization
Post-carrier primitive kernel	$(\mathcal{A}, \mathcal{H}, D, J, \Gamma, \iota_{\mathrm{C}}, P_{\mathrm{prim}}, P_{\mathrm{adm}})$, $E_3 \oplus E_2$, Y, $[u_\Sigma]$, c_3	Theorem	primitive closure kernel carrying the admissibility, carrier, and seam-normalization data before the discrete/continuous branch split
Closure data	$(\mathsf{Adm}, K_{\mathrm{adm}}, P_{\mathrm{adm}})$, (F, T), $(D_{\mathrm{geo}}, \chi_{\mathrm{geo}}, \mathcal{B}_{\mathrm{rel}}, \mathbb{A}_\Sigma)$, $(U_6, D_y, \mathcal{Y}_y^{(\varepsilon)}, \epsilon_f)$, $(Z_{\mathrm{rel}}, \Theta, \mathcal{H}_{\mathrm{rel}}, \mathcal{V}_{\mathrm{adm}})$, $(\mathcal{A}_{\mathrm{rec}}, \mathcal{A}_{\mathrm{obs}}, \mathrm{Pred})$	Derived consequence	collects the admissibility, family, geometric, transport, record, and vacuum data used by the closure theorems
Comparison layer	$\mathcal{R}_{\mathrm{cmp}}$, $\mathcal{R}_{\mathrm{SM}}$, $\alpha(0)$, M_Z, $\{m_c, m_b, m_\tau, m_t\}$	Comparison convention	translates closed outputs into scheme-specified observables, with $\mathcal{R}_{\mathrm{SM}}$ only the practical numerical preconditioner

Table 6. Core datum versus theorem, derived-consequence, and comparison-convention structures.

Symbol	First-duty meaning in the theorem chain	Status class
$\mathfrak{T}_{\partial}^{\min}$	one-sided boundary datum $(\mathcal{A}_+, \mathcal{H}_+, D_+, J, \Gamma, B_\Sigma)$	Boundary datum
$\mathfrak{T}_{\min}^{\mathrm{cl}}$	doubled closed datum $(\mathcal{A}, \mathcal{H}, D, J, \Gamma, \tau_{\mathrm{dbl}}, \iota_C)$ reconstructed from $\mathfrak{T}_{\partial}^{\min}$	Theorem
$\mathfrak{T}_{\mathrm{prim}}^{\mathrm{kin}}$	primitive kinematic scaffold $(\widetilde{M} \to M, \Sigma, \tau_{\mathrm{dbl}}, \iota_C, D_{\mathrm{ref}}, D_{\mathrm{rel}}, \chi_{\mathrm{seed}})$; when an almost-commutative realization is chosen, S and $\mathcal{H}_{\mathrm{int}}$ refer to that choice and are not additional reconstruction outputs	Theorem
$\mathcal{C}_{\min}$	minimal carrier kernel $E_3 \oplus E_2$ with one-family packet S^+	Theorem
χ_{seed}	primitive seam-even scalar response reconstructed on the primitive layer before geometric reconstruction	Theorem
σ (geometric), χ_{geo}	local Weyl conformal factor and derived local spectral scale $\chi_{\mathrm{geo}} = \Lambda e^{\sigma}$ on the geometric branch	Theorem
σ_{QCD}	QCD string tension $\sigma_{\mathrm{QCD}} = c_3^2 \chi_{\mathrm{QCD}}^2$ on the hadronic transport branch (lexically distinct from the Weyl conformal factor and from the standard-deviation σ in benchmark tables)	Theorem
$\mathrm{APS}_{\mathrm{dom}}^{\mathrm{prov}}$	provisional APS realization of the geometric anchor used in [TFPT cross-reference: `thm:well-posed-primitive-dynamics`]; an analytic starting representative	Boundary datum (analytic choice)
$\mathrm{APS}_{\mathrm{dom}}$	closed-branch APS domain obtained from $\mathrm{APS}_{\mathrm{dom}}^{\mathrm{prov}}$ by the Calderón upgrade [TFPT cross-reference: `thm:apsdom-upgrade`]	Theorem
$\mathrm{APS}_{\mathrm{fam}}$	family-pairing data induced canonically on the doubled admissible branch by the master closure roadmap	Theorem (derived)
P_{prim}	primitive admissibility projector built from ι_C, $\mathrm{APS}_{\mathrm{dom}}$, and D_{rel} alone ([TFPT cross-reference: `def:primitive-admissibility-complex`])	Theorem
$P_{\mathrm{sing}}, P_\Theta$	color-center singlet projector and determinant-sector involution projector available only after carrier and bosonic-index closure	Theorem
$\mathsf{Adm}, K_{\mathrm{adm}}, P_{\mathrm{adm}}$	admissibility predicate, positive constraint operator, and full operative selector $P_{\mathrm{adm}} = P_{\mathrm{prim}} P_{\mathrm{sing}} P_\Theta$ on the admissible branch ([TFPT cross-reference: `thm:padm-upgrade`])	Theorem
F, Ω_{adm}	topological family space and occupancy count after family closure; Ω_{adm} later feeds the closed reading of δ_{top}	Theorem
$[\nabla_F]$	$SU(3)_F$ conjugacy class of the rigid family local system used as the sole family-connection invariant in [TFPT cross-reference: `def:tfpt-rigid-pre-category`]	Theorem
δ_{ph}	unique algebraic transport root on the C_6 hexagon used on the closed branch	Theorem
Q_Θ	determinant-sector involution entering admissibility and the projector P_Θ	Theorem
$\mathcal{C}_\Sigma = \mathcal{C}_\Sigma$	*sheet-CP symmetry operator only*: $\mathcal{C}_\Sigma := CP \circ \tau_{\mathrm{dbl}}$ on the admissible branch	Theorem
T	transport generator on the family / holonomy side	Theorem
$\varpi_{\mathrm{spin}} = \varpi_{\mathrm{spin}}$	spin holonomy weight entering the geometric package	Theorem
$\mathfrak{T}_\star$	canonical rigid object of [TFPT cross-reference: `thm:no-alternatives-tfpt`]; endpoint of the theorem chain	Theorem
$\mathsf{F}_{\mathrm{fals}}(\mathfrak{T}_\star)$	structural falsification map of [TFPT cross-reference: `sec:structural-falsification-map`] (main text, hard-separated from $\mathcal{R}_{\mathrm{cmp}}$)	Theorem (side card)

Table 7. Symbol guide for theorem-level objects only. Comparison-layer and readout symbols are collected separately in Table 8. The previously colliding label $\mathcal{C}_\Sigma$ now denotes only the sheet-CP operator; seam cycle data are written $\mathfrak{C}_\Sigma$ (Table 8).

Symbol	First-duty meaning in the appendix layer	Status class
$\mathcal{R}_{\mathrm{cmp}}$	appendix-only comparison map $\mathcal{R}_{\mathrm{cmp}} : \mathfrak{T}_\star \mapsto \mathcal{R}_{\mathrm{cmp}}(\mathfrak{T}_\star)$ of [TFPT cross-reference: `sec:appendix-empirical-readout`]; never enters the theorem chain	Comparison convention
$\mathcal{R}_{\mathrm{SM}}$	practical finite-threshold numerical preconditioner used inside $\mathcal{R}_{\mathrm{cmp}}$	Comparison convention
$\mathcal{I}_{41}$	weighted abelian index $10\,b_1 = \Omega_{\mathrm{occ}}\gamma + N_\Phi$ before the closed 41 specialization (appendix bookkeeping)	Appendix bookkeeping
$\hat{m}_f$, m_f^{obs}	internal source masses and their appendix-level comparison-surface images after matching	Comparison convention
M_Σ, g_Σ	seam matching scale read from the first positive seam boundary mode and the gauge coupling evaluated there (used inside $\mathcal{R}_{\mathrm{cmp}}$)	Comparison convention
$\mathfrak{C}_\Sigma = \mathfrak{C}_\Sigma$	seam cycle data used by the matching and holonomy package; lexically distinct from the sheet-CP operator $\mathcal{C}_\Sigma$ in Table 7	Appendix-level derived data
$\mathcal{A}_{\mathrm{rec}}, \mathcal{A}_{\mathrm{obs}}, \mathrm{Pred}$	stable record algebra, observer algebra, and prediction map on the admissible sector (appendix continuation only; not part of the main theorem chain)	Appendix continuation
σ (statistical)	standard-deviation symbol used in benchmark tables for residuals (lexically distinct from the geometric Weyl factor σ and from σ_{QCD})	Appendix bookkeeping

Table 8. Symbol guide for appendix-level comparison and readout objects. These symbols never participate in the main-text theorem chain [TFPT equation: `eq:closed-output-chain`] and are recorded here only because they appear in $\mathcal{R}_{\mathrm{cmp}}$ or in the appendix bookkeeping.

Symbol	Definition	Manuscript role	First origin	Reappears in	Physical meaning
θ	seam-loop angle	core datum	seam data	a_θ	geometric rotation variable
a_θ	$\theta/(4\pi)$	hard normalization	spin lift	c_3, phase grammar	normalized cover rotation
c_3	$1/(8\pi)$	hard kernel constant	seam normalization	δ_{top}, β, σ	seam normalization constant
φ_{base}	$1/(6\pi)$	hard kernel constant	carrier geometry	φ_0^{ret}	base opening
δ_{top}	$\frac{3}{256\pi^4}$; bridge reading $\Omega_{\mathrm{adm}} c_3^4$	hard kernel value with occupancy reinterpretation	retained numerical kernel	φ_0^{ret}, δ_2	topological surcharge
φ_0^{ret}	$\frac{1}{6\pi} + \frac{3}{256\pi^4}$	retained canonical seed	retained numerical kernel	λ_Y, β, flavor	minimal nontrivial opening
γ	$\mathrm{Tr}_E\, Y^2 = 5/6$	hard kernel invariant	carrier packet	κ_{E8}, δ_2	carrier norm
B	$\mathrm{rank}\, E_3 / \mathrm{rank}\, E_2 = 3/2$	hard kernel invariant	carrier packet	δ_2	carrier rank ratio
Ω_{adm}	$3 \times 16 = 48$	closure quantity with bridge reinterpretation	APS family closure	δ_{top}	admissible chiral-state count on the family-closed branch
b_1	$\frac{4}{3} N_{\mathrm{fam}} + \frac{1}{10} N_\Phi$	hard kernel output	abelian index	benchmark map	hypercharge trace coefficient
κ_{E8}	$\gamma / \ln(248/60)$	conditional grammar	Appendix [TFPT cross-reference: `app:constants`]	scale ladder	optional scale spacing

Table 9. Constants atlas for the present manuscript.

22 Dyonic Calibration Lemma and Local $\beta_{\rm BH}(r)$ Intercept

This appendix records the analytic dyonic calibration model that supports the local achromatic intercept $\beta_{\rm BH}(r)$ used in the EHT-class residual-intercept prediction. It is a *calibration model*, not a physical horizon-scale solution: the goal is to display how the fixed TFPT coupling $1/(256\pi^4) = 16c_3^4$ is projected onto a magnetised compact-object geometry through model-dependent geometric weights.

Editorial guardrail

This is presented as a worked dyonic calibration model. It is not advertised as a parameter-free black-hole solution. The TFPT coupling is fixed; the dyonic charges, inflow geometry, and emission radius are model inputs.

22.1 Analytic dyonic toy ansatz

Consider a static, spherically symmetric ansatz with a magnetised dyonic interior and the admissible-branch axion field. Working at leading order in the boundary-normalised expansion, the axion profile, the radial electric field, and the metric function take the closed forms

$$a(r) = a_\infty + \frac{c_3\, Q_e Q_m}{8\pi^2\, r^2}, \tag{4}$$

$$E(r) = \frac{Q_e}{4\pi r^2} - \frac{c_3^2\, Q_e Q_m^2}{16\pi^3\, r^4}, \tag{5}$$

$$f(r) = 1 - \frac{2M}{r} + \frac{Q^2}{r^2} + \frac{D}{r^4}, \tag{6}$$

where $Q^2 = Q_e^2 + Q_m^2$ is the standard Reissner–Nordström-like contribution and the quartic correction D is the leading dyonic backreaction generated by the seam sector.

22.2 Local $\beta_{\rm BH}(r)$ intercept

The corresponding local rotation of the linear-polarization angle in the magnetised inflow region follows from the determinant-line / Chern–Simons response composed with the local $E\cdot B$ projection, yielding

$$\beta_{\rm BH}(r) = \frac{Q_e^{\rm eff}\, Q_m^{\rm eff}}{256\pi^4\, r^2} = 16\, c_3^4\, \frac{Q_e^{\rm eff}\, Q_m^{\rm eff}}{r^2} = \frac{\delta_{\rm top}}{3}\, \frac{Q_e^{\rm eff}\, Q_m^{\rm eff}}{r^2}, \tag{7}$$

where $Q_e^{\rm eff}(x)$ and $Q_m^{\rm eff}(x)$ encode the local effective dyonic weights in the bright magnetically dominated regions of the horizon-scale image, and $\delta_{\rm top} = 48c_3^4$ is the topological coefficient of the α-kernel correction. The coupling in front is fixed by the same TFPT branch data that fixes α and $\beta_{\rm rad}$; the spatial weights are MHD/GR inputs of the source model.

22.3 Horizon-shift sign correction

A known wording slip in earlier draft notes describes the $D > 0$ shift of (6) as a "microscopic increase" of the outer horizon. This is reversed by direct inspection of the quartic term: with $D > 0$, the function $f(r)$ acquires a positive contribution that grows as $1/r^4$, so the outer root of $f(r) = 0$ migrates inward.

Lemma 22.1 (Horizon shift sign). *Let $f_0(r) = 1 - 2M/r + Q^2/r^2$ have outer horizon $r_+^{(0)}$. For $f_D(r) = f_0(r) + D/r^4$ with $D > 0$ small enough that the outer real positive root persists, the shifted outer horizon $r_+(D)$ satisfies*

$$r_+(D) \;<\; r_+^{(0)}.$$

The sign of the dyonic correction therefore decreases *the radius of the outer horizon, not increases it, in this regime.*

Proof. Implicit differentiation of $f_D(r_+(D)) = 0$ gives

$$\frac{dr_+}{dD} = -\frac{1/r_+^4}{f_0'(r_+) + (\partial_r D/r^4)|_{r_+}}.$$

At the outer horizon f_0 crosses zero from below to above with $f_0'(r_+^{(0)}) > 0$, so the denominator is positive at $D = 0$ and the numerator is positive, giving $dr_+/dD < 0$. □

22.4 Calibration scope

Remark (What this lemma is not). Equation (7) is presented as an *analytic dyonic calibration lemma*. It is not advertised as a realistic black-hole solution and does not replace a full GRMHD/synchrotron forward model. Its only purpose in the TFPT layer is to display the structural $1/r^2$ profile and the fixed coupling $1/(256\pi^4)$ that enter the achromatic residual intercept of the linear polarization angle.

23 External RG Fingerprint Protocol

This appendix records an external stress-test protocol for the closed-branch admissibility data, formulated as a set of RG fingerprints to be reproduced by an independent two-loop renormalisation solver (e.g. PyR@TE) seeded with the TFPT input package. The fingerprints are *external comparison* targets, not internal theorem claims: their purpose is to give a sceptical reader a clean numerical reproduction surface.

Editorial guardrail

The RG fingerprints are presented as an external comparison protocol, not as primitive input. They become trustworthy only after independent two-loop reproduction with the declared configuration; until then they are a planned compass with no fixed north.

23.1 TFPT branch input package

The configuration handed to the external solver freezes the closed-branch admissibility data

$$c_3 = \frac{1}{8\pi}, \qquad \varphi_0^{\mathrm{ret}} = \frac{1}{6\pi} + \frac{3}{256\pi^4}, \qquad \alpha^{-1}(0) = 137.0359992168\ldots, \qquad b_1 = \frac{41}{10},$$

together with the carrier rank data $(\dim E_-, \dim E_+) = (3,2)$, family multiplicity $N_{\mathrm{fam}} = 3$, admissible occupancy $\Omega_{\mathrm{adm}} = 48$, and Higgs index $N_\Phi = 1$ from Paper 2. The two-loop SM running is performed inside the standard $(g_1, g_2, g_3, y_t, \lambda)$ system with the declared threshold map.

23.2 Four fingerprints

The fingerprint targets to be reproduced by the external solver are:

1. **Strong-coupling crossing at the seed value.** On the canonical branch the two-loop strong coupling crosses φ_0^{ret} at PeV scales,
$$\alpha_3(\mu_1) \approx \varphi_0^{\mathrm{ret}}, \qquad \mu_1 \approx 1\,\mathrm{PeV}.$$

2. **Strong-coupling crossing at the seam constant.** It crosses c_3 in the intermediate corridor,
$$\alpha_3(\mu_2) \approx c_3, \qquad \mu_2 \approx 2.5\times 10^8\,\mathrm{GeV}.$$

3. **G8 bridge.** Above
$$M_{G8} \approx 1.8\times 10^{10}\,\mathrm{GeV}$$
the boundary-polarised admissibility data permits a G8 bridge as a downstream scale-grammar interface, not as a primitive new particle. The bridge feature is at the level of slope grammar, not of phenomenological resonances.

4. **Unification corridor.** The three SM gauge couplings approach a unification corridor at
$$\mu_{\mathrm{unif}} \approx 1.43\times 10^{15}\,\mathrm{GeV}, \qquad \left.\frac{\Delta\alpha_i}{\alpha_i}\right|_{\mathrm{spread}} \approx 1.23\%.$$

23.3 Status discipline

Remark (Fingerprints, not theorems). The four items above must be presented as *external comparison fingerprints* of the closed branch through standard SM running, not as new theorem-level claims. They are reproducible from a declared PyR@TE configuration that uses only the upstream TFPT inputs listed above. Until that reproduction is published as a companion artifact, the fingerprints are programmatic targets.

Remark (E8 as downstream scale grammar). The G8 bridge of fingerprint 3 is recorded at the level of scale grammar inherited from the E8 discussion of the source draft. It is *not* reintroduced as a primitive cause in the boundary kernel; the boundary-polarised closed branch already determines α, the carrier rank, the family count, and the admissibility complex without invoking E8 as an upstream input.

24 Source Extraction Map

Source extraction map

Use `../tfpt-42.tex`:

- Appendix-level empirical readout sections.
- Technical conventions and data layers.
- Constants atlas and downstream scale grammar.
- Relative APS and superconnection setup.
- Relative reflection positivity with fermions.
- Admissible OS reconstruction and asymptotic scattering.
- FRW reduction and cosmology interface proofs.
- Yukawa kernels and positivity lemmas.
- Information-theoretic and cut-and-project readings.
- Record algebra and pointer dynamics.
- Horizons, modular flow, and black hole thermality.
- Prediction semantics and transient event channels.
- Closed theoretical outputs and empirical comparison surface.
- Extended benchmarks and novelty boundary.

25 Promotion Rule

If a companion item becomes load-bearing for a theorem paper, it must be promoted into that paper's technical backend or cited as a named standard-theorem interface. The companion should never be the place where a major assumption first becomes invisible.